PNL-4742

NUREG/CR-3317
PNL-4742
R1

Technical Bases and User's Manual for the Prototype of a Suppression Pool Aerosol Removal Code (SPARC)

Prepared by P. C. Owczarski, R. I. Schreck, A. K. Postma

Pacific Northwest Laboratory
Operated by
Battelle Memorial Institute

Prepared for
U.S. Nuclear Regulatory Commission

NUREG/CR-3317
PNL-4742
R1

Technical Bases and User's Manual for the Prototype of a Suppression Pool Aerosol Removal Code (SPARC)

Manuscript Completed: April 1985
Date Published: May 1985

Prepared by
P. C. Owczarski, R. I. Schreck, A. K. Postma

Pacific Northwest Laboratory
Richland, WA 99352

Prepared for
Division of Engineering Technology
Office of Nuclear Regulatory Research
U.S. Nuclear Regulatory Commission
Washington, D.C. 20555
NRC FIN B2444

NUREG/CR-3317
PNL-4742
R1

Technical Bases and User's Manual for the Prototype of a Suppression Pool Aerosol Removal Code (SPARC)

Manuscript Completed: April 1985
Date Published: May 1985

Prepared by
R. C. Owczarski, R. J. Schreck, A. K. Postma

Pacific Northwest Laboratory
Richland, WA 99352

Prepared for
Division of Engineering Technology
Office of Nuclear Regulatory Research
U.S. Nuclear Regulatory Commission
Washington, D.C. 20555
NRC FIN B2444

PREFACE

The prototypic version of the pressure Suppression Pool Aerosol Removal Code (SPARC) has been used by several organizations. The code was released in 1983 for use in the formulation of a systematic, mechanistic approach for estimating the source terms of severe accidents at nuclear power plants (Gieseke et al. 1984). This document supporting the prototype version of SPARC is being published now so that the information used in that effort will be publicly available.

A draft document describing an updated version of SPARC is now being prepared. The newer version of SPARC includes improved descriptions of condensational particle growth and deposition velocities of particles inside rising bubbles.

ABSTRACT

The Pacific Northwest Laboratory has developed a prototypic version of a Suppression Pool Aerosol Removal Code (SPARC). This code was written to calculate the capture of aerosol particles in the pressure suppression pool (wet well) of a boiling water reactor under hypothetical accident conditions. The code incorporates five aerosol scrubbing models and two thermal-hydraulic models. The scrubbing models describe 1) steam condensation, 2) soluble particle growth in a humid atmosphere, 3) gravitational settling, 4) inertial deposition, 5) diffusional deposition. Mechanical entrainment of pool liquid by breaking of bubbles at the surface was also considered. An optional model for equilibrium pool temperature and a model for steam evaporation are the two thermal-hydraulic models used in the code. Steam evaporation was found to significantly retard deposition processes in pools near the boiling point.

The code user supplies the values of several controlling variables in the code input. The SPARC output can include the decontamination factors (DF) of twenty different particle size groups, an overall DF for the whole particle distribution, particle log normal distribution parameters, and mass flow rates of particles (wet and dry) leaving the pool.

SUMMARY

In a program for the U.S. Nuclear Regulatory Commission, the Pacific Northwest Laboratory developed a prototypic version of a Suppression Pool Aerosol Removal Code--SPARC. The computer code was written to calculate the depletion of aerosol particles in the pressure suppression pool (wet well) of a boiling water reactor under hypothetical accident conditions. This report briefly describes the technical bases of the code (the models used) and gives instructions for its use.

The code incorporates five aerosol scrubbing models and two thermal-hydraulic models. The aerosol scrubbing process is described by

- convective flows from the condensation of steam
- growth of soluble particles by water vapor sorption
- gravitational settling (sedimentation)
- inertial deposition due to circulation of the bubble surface
- diffusional deposition.

Descriptions of these models are first expressed for spherical bubbles and then for oblate spheroid bubbles. The model for particle growth in nearly saturated atmospheres is particularly important. This particle growth is due to the deliquescence of soluble fractions of the dry particles in the humid atmosphere of a bubble rising through the pool liquid. Mechanical entrainment of pool liquid by bubbles breaking at the pool surface is also considered.

The thermal-hydraulic models consist of two parts. The first part is the model for the equilibrium pool temperature. This is the steady-state temperature of the pool in thermal and vapor equilibrium with the gas leaving the pool. The gas contains noncondensible hydrogen, air, carbon monoxide and/or carbon dioxide, as well as water vapor and scrubbed particles. The second part is the model for steam evaporation into the bubble as it rises. This incoming steam is the result of the steam maintaining vapor equilibrium as the bubble rises. This steam influx retards all particle deposition mechanisms, and it is especially important in pools near the boiling point.

The code follows an aerosol of 20 discrete particle sizes as the particles deposit on the bubble walls by the various mechanisms. The output components of SPARC are the particle decontamination factors and the log normal distribution parameters of the outlet aerosol. To operate the code, the user must input these parameters:

- mass flow rates of the gases
- concentration of each particle size class entering the pool

- soluble fraction and density of the particles
- pressure and temperature of inlet gases
- depth and temperature of the suppression pool (An option is available to use a code-calculated equilibrium pool temperature.)
- initial bubble size and shape
- desired output times.

The discussion of the model's use includes a sample problem to illustrate the input and output of SPARC.

Although a number of parameter sensitivity studies have been carried out with SPARC, this report contains only one set of these, concerning bubble shape. The effect of bubble shape is shown to have a marked effect. The more flattened the bubble is, the more effective all the deposition mechanisms are. Other parameters having an effect on decontamination factors are: bubble size, particle size, fraction soluble material, particle density, pool temperature, pool depth, pressure above the pool, and noncondensible carrier gas species.

TABLE OF CONTENTS

FIGURES

TABLES

GLOSSARY OF SYMBOLS

a	radius of spherical bubble
a	major axis of elliptical cross section
A_s	surface area (of bubble)
b	minor axis of elliptical cross section
C_m	Cunningham slip correction factor
C_p	heat capacity
C_{vb}	bulk bubble vapor concentration
C_{vo}	vapor concentration at the interface
d_p	particle diameter
D	bubble diameter or equivalent sphere diameter
$\mathcal{D}$	particle diffusivity
DF	decontamination factor: ratio of mass entering to that escaping from the suppression pool
DF_D	decontamination factor due to diffusion
D_h	bubble diameter at water depth h
D_s	bubble diameter at the surface of the pool
D_{vB}	molecular diffusivity of vapor in noncondensible gas B
e	eccentricity
F	volume fraction of inlet gas condensed
F_c	centrifugal force
F_d	drag force
g	acceleration due to gravity
G	gas flow rate
h	downcomer submergence depth
h	specific enthalpy of gas
Δh	effective bubble rise distance
h_l	specific enthalpy of pool liquid
h_c	specific enthalpy change due to evaporation (latent heat of evaporation)
i	Van't Hoff ionization factor
k	Boltzmann's constant
K_c	Rate constant for centrifugal deposition
K_D	rate constant for diffusional deposition
K_s	rate constant for sedimentation
m	mass (of solute in a drop or of particle)
M	molecular weight (of solute)
M	total mass of water in the pool
M_g	moles of noncondensible gas
M_o	molecular weight (of solvent)
Mw	average molecular weight at the surface
n_L	numbers of molecules/cm^3 of solution (solvent + solute)
N_n	noncondensible moles per bubble
N_v	moles of vapor in bubble (at depth h)

N_v^s moles of vapor in bubble at the pool surface
p atmospheric pressure above pool
P_s total pressure at pool surface
P_t total pressure at gas inlet
P_T total atmospheric pressure above pool
P_w water vapor pressure
q average heat flux to the interface
Q decay heat due to fission products contained in pool water
r radius of curvature
R gas constant
R_a ratio of major and minor ellipse axes (a/b)
S saturation ratio
t_e exposure time
Δt residence time of bubble in the pool
T gas or pool temperature
T_b bulk pool temperature
T_o interface temperature
T_w gas temperature in bubble
U bubble swarm rise velocity
v_b bubble rise velocity
v_c drift velocity due to centrifugal force
v_{cm} maximum centrifugal drift velocity
v_D deposition velocity due to diffusion
v_p peripheral velocity (of gas in a rising bubble)
V bubble volume
V_o original bubble volume at depth where stable bubble sizes are first formed
V_d net deposition velocity
V_s particle settling velocity
V_v gas bulk flow velocity due to steam evaporation
W_v average flux of vapor into a bubble
X mole fraction of noncondensible gas (e.g., hydrogen in inlet gas)
X_i mole fraction of noncondensibles in inlet gas
X_o mole fraction of noncondensibles in inlet gas bubble after it attains thermal equilibrium in the suppression pool
y^* multiplier relating v_c in a spherical bubble to v_c in an oblate spheroid
Y_h mole fraction of vapor (at depth h)
Y_s mole fraction of vapor (at pool surface)

Greek Symbols

α water thermal diffusivity
Δh effective bubble rise distance
Δt residence time of bubble in the pool
Θ correction factor for high mass transfer rates
μ gas viscosity

ρ	water or solution density
ϕ	a flux ratio

Subscripts and Superscripts

0	zero denotes conditions applicable to the original bubble at a water depth where stable bubble sites are first formed
'	prime denotes values adjusted for an oblate spheroid bubble
i	refers to inlet gas
o	refers to outlet gas

1.0 INTRODUCTION

The U.S. Nuclear Regulatory Commission is studying the effectiveness of Engineered Safety Features (ESFs) in light water reactors under postulated severe accident conditions. These conditions are those that could result from a highly degraded core and possible interactions between the core and the concrete basemat. Elevated temperatures, high pressures, and very high aerosol concentrations (up to 10 g/m^3) might be characteristic of the reactor containment atmospheres under these conditions. The responses of the ESFs to the severe conditions will be examined both by modeling and by experiments. Early goals are to obtain models of aerosol behaviors in ESFs such as pressure suppression pools, ice condensers, containment sprays, and filtration systems.

The Pacific Northwest Laboratory has produced a prototypic Suppression Pool Aerosol Removal Code (SPARC) that contains several models for aerosol particle depletion and thermal hydraulics. This new computer code is being developed to calculate the capture of aerosol particles by the wet well (pressure suppression pool) of a boiling water reactor (BWR) for hypothetical accidents in which aerosols from a degraded core or core/concrete reaction are forced through the pool. The code's models use currently available theories for making these calculations. The ultimate goal is to improve available theory and calculational methods with new experiments suggested by the models in the code itself. Plans for continuing code development are described in Section 2 of this document.

The objectives of this document are to review the technical bases of SPARC, describe the code, and give instructions for its use. Section 3 covers the technical bases of the code--the aerosol scrubbing models and the thermal hydraulic models. Section 4 describes SPARC's operating requirements and includes sample problems to demonstrate the code's input and output. An appendix lists the prototypic version of SPARC.

2.0 CONTINUING CODE DEVELOPMENT

The prototypic version of SPARC described in this report includes five aerosol scrubbing models and two thermal-hydraulic models. SPARC will be continually improved as more experimental information is made available. The first improvements will be the inclusion of better definitions of bubble size and shape to represent the real distribution present in a swarm of bubbles in a pool. These will include a shape factor as a function of bubble size, and bubble size as a function of inlet steam concentration. The addition of subroutines to predict the extent of growth of aerosol particles by condensation in a supersaturated atmosphere is also planned. Two of the major unknowns are the roles of surfactants and pool debris on the circulation of the drops. Only experimental programs will provide quantitative information on these parameters. Validation of SPARC will be a continuing process. The major plans are to compare SPARC calculations with the data and calculations obtained by programs now being sponsored by the Electric Power Research Institute (EPRI).

3.0 TECHNICAL BASES FOR SPARC

This chapter briefly describes each model used in SPARC. References are supplied for the reader who wants additional details. The models are found in two groups: aerosol scrubbing models and thermal-hydraulic models.

3.1 AEROSOL SCRUBBING MODELS

The models developed herein start with a "bubbling" model described by Fuchs (1964). In the Fuchs model, the dominant scrubbing processes take place inside rising bubbles. These scrubbing processes are discussed in the following section. Extensions of these processes using optional equations for oblate spheroid bubbles are presented in Section 3.1.2.

3.1.1 Scrubbing Processes and Related Phenomena

Several physical processes are involved in transporting gas-borne particles to the liquid interface (bubble surface) when steam/gas mixtures are bubbled through a water pool. The following processes have been accounted for in the SPARC scrubbing model:

1. convective flows resulting from the condensation or evaporation of steam

2. particle growth caused by water vapor sorption by soluble aerosol material

3. sedimentation resulting from gravitational forces

4. inertial deposition resulting from centrifugal forces

5. diffusional deposition

6. mechanical entrainment of pool liquid by the breaking of bubbles at the surface.

The technical bases and predictive equations used for each of these processes are described in the following sections.

Convective Flow Effects

The condensation of steam from the carrying gas represents a convective flow towards the water surface. This flow will enhance particle capture. On

the other hand, the evaporation of water into a bubble represents a convective flow that retards particle deposition.

Condensation, if any takes place, would be expected to occur near the gas entry point into the pool. It is assumed that the gas attains thermal equilibrium with pool water in the immediate vicinity of the entry point. Thus an inlet scrubbing factor applicable to the bubble forming processes can be estimated on the basis of the fraction of the gas that condenses. It is assumed that the particles are swept along with the condensing steam. The removal efficiency is:

fractional efficiency = fraction condensed.

Numerically, the fraction of the inlet gas that is condensed can be expressed in terms of the mole fraction of noncondensible gas:

$$F = 1 - \frac{X_i}{X_o} \tag{3.1}$$

where F = volume fraction of inlet gas condensed
X_i = mole fraction of noncondensibles in the inlet gas
X_o = mole fraction of noncondensibles in the gas bubble after it attains thermal equilibrium in the pool near the inlet location.

F, the fractional removal efficiency, may be expressed as a decontamination factor (ratio of mass entering to that escaping from the pool). A DF applicable to all particle sizes may be obtained by rearranging Equation (3.1):

$$DF = \frac{1}{1 - F} = \frac{X_o}{X_i} \tag{3.2}$$

The numerical values of X_i can be expected to vary with time and therefore are treated as an input quantity. The value of X_o, on the other hand, is fixed by pool temperature (fixed water vapor pressure) and total pressure. X_o may be expressed as:

$$X_o = 1 - \frac{P_w}{P_t} = 1 - \frac{P_w}{p + \rho g h} \tag{3.3}$$

where P_w = vapor pressure or water
P_t = total pressure at gas inlet
P_T = atmospheric pressure above pool
ρ = water density
g = gravity acceleration
h = downcomer submergence depth.

Condensation will occur if X_o is greater than X_i; otherwise evaporation will occur and the vapor flux will retard particle motion toward the interface. For $X_o < X_i$ it is assumed that no deposition occurs, i.e., that DF = 1.

Once a bubble begins to rise, evaporation will begin because the pressure inside the bubble decreases with decreasing depth. The number of moles of noncondensible gas that are contained within a single bubble may be computed from the ideal gas law as:

$$M_G = \frac{X P_t V}{R T_w} \tag{3.4}$$

where X = mole fraction on noncondensible gas
M_G = moles of noncondensible gas
P_t = total pressure
V = bubble volume
R = gas constant
T_w = gas temperature in bubble, assumed to be the same as the water temperature.

A good approximation is that the moles of noncondensible gas (H_2, CO_2, etc.) in a single bubble will remain constant. If M_G is assumed to be constant, and if water vapor pressure is assumed to be constant, then Equation (3.4) can be used to compute the bubble volume as a function of depth (depth determines total pressure):

$$\frac{V}{V_o} = \frac{X_o P_{to}}{\left(1 - \frac{P_w}{P_t}\right) P_t} \tag{3.5}$$

The o subscripts in Equation (3.5) denote conditions applicable to the original bubble at a water depth where stable bubble sizes are first formed. This is the downcomer submergence minus the distance required for bubble shattering. Inspection of Equation (3.5) shows that V/V_o will be greater than unity because P_t, the total gas pressure, decreases as the bubble rises. An example calculation illustrates predicted growths: for an inlet gas at 500°C containing 20% hydrogen, the pool is calculated to reach a steady-state

temperature of 95.5°C (one atmosphere pressure above the pool). For an initial bubble depth of 7 feet, Equation (3.5) predicts a volume ratio of 3.8. Most of the increased volume is water vapor, and the water vapor flux entering from the liquid interface retards particle deposition.

Step-by-step calculations show that the steam inflow velocity is a minimum at the entry point into the pool and increases as the bubble rises. Thus the retarding effect on particle deposition varies with bubble depth. This variation with depth requires that the scrubbing model account for scrubbing efficiency as a function of bubble depth. Mass and heat transfer resistances hinder the steam inflow velocity. See Section 3.2.2 for details of this effect.

Particle Growth by Water Vapor Uptake

The gas inside rising bubbles will be nearly saturated with water vapor. This humid atmosphere is conducive to the growth of soluble particles by water vapor uptake.

The equilibrium drop size reached in a humid atmosphere is governed by the degree to which the vapor pressure of water is lowered by the soluble material, and the degree to which decreasing droplet size effects an increase in the vapor pressure. Both effects are well understood and are calculable using classical physics and chemistry. The equilibrium saturation ratio , S, is related to drop size by an equation presented by Fletcher (1962):

$$S = \frac{\exp\left[\frac{2\sigma}{n_L KTa}\right]}{\left[1 + \frac{imM_o}{M\left(\frac{4}{3}\pi a^3 \rho - m\right)}\right]} \qquad (3.6)$$

where S = saturation ratio (the relative humidity)
σ - surface tension of solution
n_L = number of molecules/cm^3 of solution (solvent + solute)
k = Boltzmann's constant
T = temperature, °K
a = radius of drop
i = Van't Hoff ionization factor
ρ = density of solution
M = molecular weight of solute
M_o = molecular weight of solvent
m = mass of solute in the drop.

Equation (3.6) was evaluated under the assumption that the solute was cesium hydroxide, the solvent was water, and the temperature was 100°C. Results are summarized in Table 1.

The data of Table 1 illustrate that particle growth factors depend on the relative humidity, S, and that significant growth factors are predicted.

Because the drop size/particle size ratio depends strongly on the relative humidity, a first estimate of relative humidity inside a bubble was made. This was done by computing the concentration gradient required to produce the water vapor flux that would be required to maintain saturation in a rising bubble. For a bubble submerged initially 10 ft in a water pool at 99°C, an average steam evaporation velocity of 0.0304 cm/s was calculated for the first second of rise time. For a bubble containing H_2 as the inert gas, S in the bulk of the bubble was calculated to have a value of 0.993; for a bubble containing CO_2, S was estimated to have a value of 0.985. Based on these two estimates, it appears that an S value of 0.99 would be a reasonable first-estimate value. Equilibrium droplet radii listed in Table 1 for this relative humidity indicate that water uptake causes growth by roughly a factor of 4. This amount of growth could have an important effect on the overall OF because it would move particles from the most penetrating range (0.1 to 1.0 μm) into larger size ranges that are more efficiently collected.

Particle Capture by Sedimentation

Gravitational forces cause particles to settle. Capture by this process is termed sedimentation. The depletion rate is expressible as:

depletion rate = (airborne concentration)(velocity)(area)

The velocity-area product varies with position along the bottom part of the bubble, and hence must be evaluated by integration. The net downward velocity and incremental horizontal areas for a spherical geometry are illustrated in Figure 1.

TABLE 1. Growth of CsOH Particles in Humid Atmosphere at 100°C

Dry Particle Radius, μm	Droplet Radius in Stated Humidity, μm			
	S=0.9	S=0.95	S=0.99	S=0.999
0.01	0.0195	0.0225	0.295	0.0345
0.10	0.195	0.255	0.425	0.775
1.0	1.95	2.55	4.45	9.35
10.0	19.5	15.5	44.5	95.5

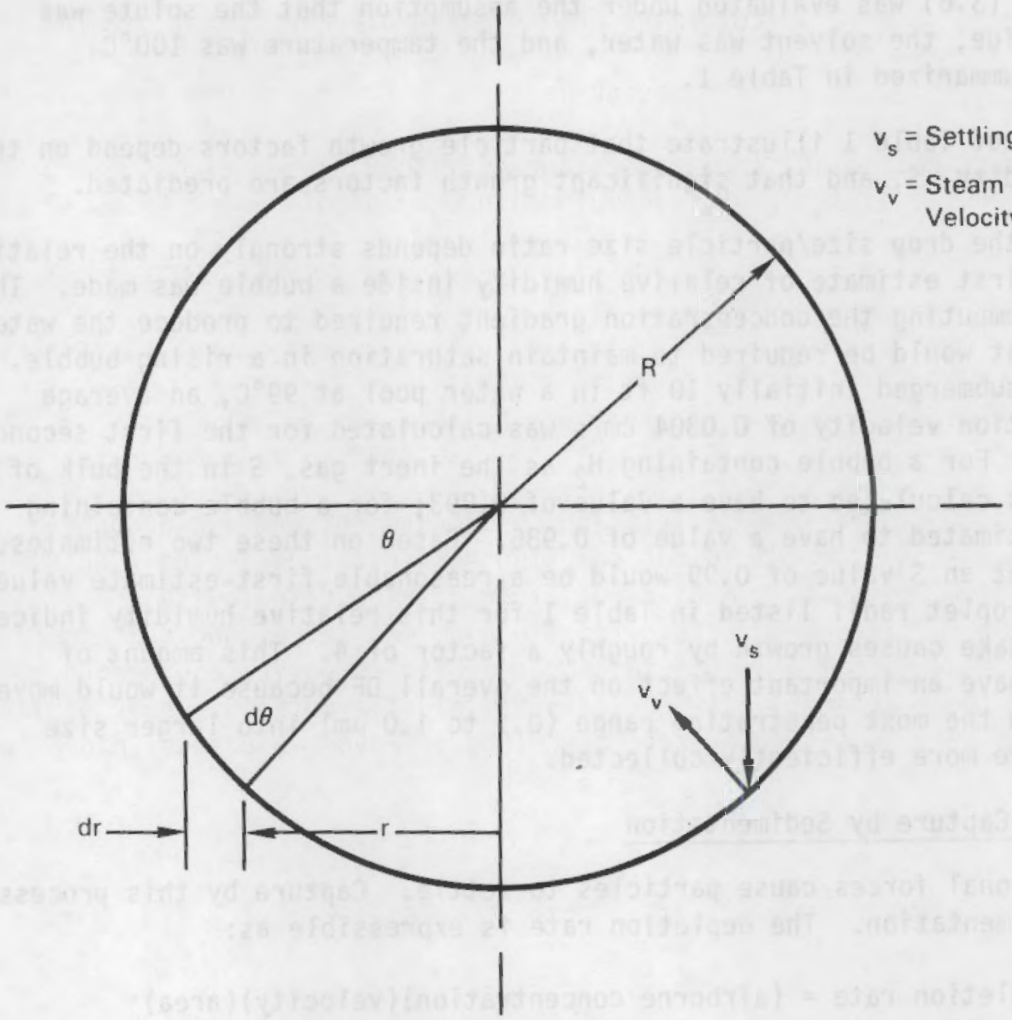

FIGURE 1. Sedimentation in a Spherical Bubble

For small spherical particles in a low-density medium the Stokes velocity applies for the settling velocity, v_s (Bird, Stewart and Lightfoot 1960):

$$v_s = \frac{\rho_p \, d_p^2 \, C_m \, g}{18\mu} \qquad (3.7)$$

where ρ_p = particle density
d_p = particle diameter
C_m = Cunningham slip correction factor
g = acceleration due to gravity
μ = gas viscosity.

The net downward velocity at the periphery of the spherical bubble is the vector sum of the settling velocity and the inward steam velocity:

$$v = v_s - v_v \sin\theta \tag{3.8}$$

Deposition becomes zero when v = 0. If v is set equal to zero, and Equation (3.8) is solved for θ, the result is:

$$\theta_m = \arcsin\left(\frac{v_s}{v_v}\right) \tag{3.9}$$

The value of θ_m defined in Equation (3.9) sets the upper limit for the integration of deposition velocity times area over angle θ.

The incremental horizontal area described by a radius at angle θ is expressible as follows:

$$dA = 2\pi R^2 \cos\theta \sin\theta d\theta \tag{3.10}$$

The integral of deposition velocity times area may be written by using Equations (3.8) through (3.10):

$$\int_0^{\theta_m} vdA = \int_0^{\arcsin\left(\frac{v_s}{v_v}\right)} (v_s - v_s \sin\theta)(2\pi R^2 \cos\theta \sin\theta d\theta) \tag{3.11}$$

Carrying out the integration indicated in Equation (3.11) yields, after algebraic simplifications,

$$\int_0^{\theta_m} vdA = \pi R^2 \left(\frac{v_s}{v_v}\right)^2 \left[v_s - \frac{2v_v}{3}\frac{v_s}{v_v}\right] \tag{3.12}$$

subject to the condition:

$$0 < \frac{v_s}{v_v} < 1 \tag{3.13}$$

For v_s/v_v values greater than unity, v_s/v_v must be set equal to unity. This constraint arises from the fact that the maximum meaningful value for θ is $\pi/2$.

The aerosol depletion rate in a single bubble may be obtained by multiplying the aerosol concentration (bubble assumed to be perfectly mixed) by the area deposition velocity product defined in Equation (3.12). A decontamination factor that results after time Δt is found to be

$$DF = \exp\left\{\frac{3\Delta t}{2D}\left[v_s - \frac{2}{3}v_v\left(\frac{v_s}{v_v}\right)\right]\left(\frac{v_s}{v_v}\right)^2\right\} \qquad (3.14)$$

where DF = decontamination factor due to sedimentation
Δt = residence time of the bubble in the pool
D = bubble diameter
v_s = particle settling velocity
v_v = gas bulk flow velocity due to steam evaporation.

Equation (3.14) is subject to the constraint defined by Equation (3.13).

Particle Capture by Centrifugal Forces

Bubbles larger than a critical size experience surface circulation as they rise through liquid (Calderbark and Lochiel 1964). If retarding effects due to interfacial contaminants are neglected, then the peripheral velocity, v_p, can be related to rise velocity by assuming potential flow around a sphere (Fuchs 1964):

$$v_p = 1.5\, v_b \sin\theta \qquad (3.15)$$

where the angle θ is measured from the vertical pole.

The peripheral velocity induces a centrifugal force on particles in gas located near the bubble wall:

$$F_c = \frac{m v_p^2}{r} \qquad (3.16)$$

where F_c = centrifugal force
m = mass of particle
r = radius of curvature
v_r = peripheral velocity.

This centrifugal force produces a particle drift velocity whose magnitude is such that centrifugal force is balanced by drag force. From Stokes' law, the drag force is related to drift velocity by

$$F_d = \frac{3\pi d_p \mu v_c}{C_m} \tag{3.17}$$

where F_d = drag force
d_p = particle diameter
μ = gas viscosity
v_c = drift velocity due to centrifugal force
C_m = Cunningham slip correction factor.

The drift velocity (v_c) with respect to the bulk gas motion, may be obtained from Equations (3.15) through (3.17) as

$$v_c = \frac{9}{2} \frac{v_b^2 \, v_s \, \sin^2\theta}{D \, g} \tag{3.18}$$

and the net deposition velocity compared to fixed coordinates (the bubble interface) is

$$v_d = v_c - v_v \tag{3.19}$$

where v_d = net deposition velocity
v_c = drift velocity due to centrifugal force
v_d = bulk flow velocity normal to the interface resulting from steam evaporation.

Deposition will begin when v_d first takes a positive value. The angle at which this would occur is predictable from Equations (3.19) and (3.18) by setting $v_c = 0$. The result is

$$\theta_1 = \arcsin\left(\frac{4D\mu v_v}{v_v^2 \rho_p d_p^2 C_m}\right) \tag{3.20}$$

where θ_1 = angle at which centrifugal velocity and bulk flow velocity are equal in magnitude and opposite in direction.

The argument of the arcsin function in Equation (3.20) may be expressed as a velocity ratio:

$$\frac{4D\mu v_v}{v_v^2 \rho_p d_p^2 C_m} = \frac{v_v}{v_{cm}} \tag{3.21}$$

where v_{cm} = maximum centrifugal drift velocity (at $\Theta = \pi/2$).

The overall deposition rate may be obtained by integrating the product of net deposition velocity and deposition area from ($\Theta = \Theta$) to ($\Theta = \pi - \Theta_1$). The result of such an integration is:

$$\text{deposition velocity} \cdot \text{area} = \pi D^2 v_{cm} \left(1 - \frac{v_s}{v_{cm}}\right)\left(\frac{2}{3} + \frac{v_s}{v_{cm}}\right) \tag{3.22}$$

subject to the constraint that $v_s/v_{cm} < 1$.

For a single bubble of constant volume, the aerosol deposition rate predicted by Equation (3.22) leads to the following decontamination factor for centrifugal deposition.

$$DF = \exp\left[\frac{6v_{cm}}{D}\left(1 - \frac{v_v}{v_{cm}}\right)^{\frac{1}{2}}\left(\frac{2}{3} + \frac{v_v}{v_{cm}}\right)\right]\Delta t \tag{3.23}$$

Equation (3.23) is subject to the constraint that v_v/v_{cm} is unity or smaller. For cases where v_v/v_{cm} is calculated to be larger than unity, the ratio should be set equal to unity, resulting in a DF of unity.

Diffusional Deposition

Particles have a finite diffusivity as a result of momentum exchanges with surrounding gas molecules. Particles diffusivity may be related to gas and particle properties by the Stokes - Einstein Equation (Fuchs 1964):

$$\mathcal{D} = \frac{kTC_m}{d\pi\mu} \tag{3.24}$$

where $\mathcal{D}$ = particle diffusivity
k = Boltzmann's constant.

The rate of diffusional deposition onto the bubble wall may be computed from the penetration theory of mass transfer (Bird, Stewart and Lightfoot 1960; Crank 1967). The mass transfer coefficient (deposition velocity) may be expressed as

$$v_D = 2\left(\frac{\mathcal{D}}{\pi t_e}\right)^{1/2} \tag{3.25}$$

where v_D = deposition velocity due to diffusion
t_e = exposure time.

An estimate of exposure time for a circulating bubble may be obtained by dividing bubble diameter by rise velocity (Li et al. 1965):

$$t_e = \frac{D}{v_b} \tag{3.26}$$

Combining Equations (3.19) and (3.20) leads to

$$v_D = 2\left(\frac{\mathcal{D}v_b}{\pi D}\right)^{1/2} \tag{3.27}$$

This deposition velocity applies when the vapor flux at the wall is negligible. Deposition is reduced by the steam flux entering a rising bubble. A correction factor for high mass transfer rates can be estimated from the data presented by Bird, Stewart and Lightfoot (1960). Using the penetration theory, we can relate a correction factor Θ to a flux ratio:

$$\Theta = (1 + \mathrm{erf}\phi)^{-1}\exp(-\phi^2) \tag{3.28}$$

where Θ = correction factor for high mass transfer rates
ϕ = a flux ratio.

The flux ratio ϕ is equal to ϕ_{AB}/π where ϕ_{AB} is defined as

$$\phi_{AB} = \frac{v_v}{2\left(\frac{\mathcal{D}v_b}{\pi D}\right)^{1/2}} \tag{3.29}$$

For small values of ϕ_{AB} (low v or high D), Θ approaches unity; Θ approaches zero for high values of ϕ_{AB}. If the deposition velocity as defined in Equation (3.21) is multiplied by Θ, and the net velocity is applied over the whole bubble surface, a DF due to diffusion is expressible as:

$$DF_D = \exp\left[\frac{12\Theta}{D}\left(\frac{\rho v_b}{\pi D}\right)^{1/2} \Delta t\right] \tag{3.30}$$

Overall DF

A common term in the three DF expressions [Equations (3.30), (3.23), and (3.14)] is the bubble residence time, Δt. This time is equal to the rise distance divided by the swarm rise velocity:

$$\Delta t = \frac{\Delta h}{U} \tag{3.31}$$

where Δh = effective bubble rise distance
U = swarm rise velocity.

The overall DF due to the four mechanisms characterized by Equations (3.2), (3.14), (3.23), and (3.30) may be expressed as a product:

$$DF = \frac{X_o}{X_i} \exp\left[(K_s + K_c + K_p)\Delta t\right] \tag{3.32}$$

where X_o/X_i = DF for steam condensation (DF < 1)
K_s = first order rate constant for sedimentation from Equation (3.14), $K_s > 0$
K_c = first order rate constant for centrifugal deposition from Equation (3.23), $K_c > 0$
K_D = first order rate constant for diffusional deposition from Equation (3.30).

Obvious assumptions in the derivation presented above include the following:

- Bubbles are spheres having a circulation velocity unimpeded by interfacial contaminants.
- Particles are solid spheres; for nonspheres, appropriate shape factors would have to be specified.

- The DF is a function of particle size; an overall DF would have to be integrated over the particle size distribution.

- The degree of particle growth depends on the fraction of the particle mass that is soluble; thus the soluble fraction will have to be specified.

Entrainment

When bubbles break up at the pool surface, aerosol particles are formed from the remnants of the liquid film of the bubble's upper surface. To quantify this phenomenon correctly would require an inventory of previously scrubbed material in the pool. Since this inventory is a possible future development for SPARC, a simpler alternative was to limit the maximum DF for any particle size to 10^5 in the prototype of SPARC. This limit is a very crude estimate made by using a fully (in one hour) contaminated pool with an entrainment of 10^{-3}%/hr.

3.1.2 Optional Equations for Oblate Spheroid Bubbles

The largest number of bubbles in a swarm are flattened spheres (oblate spheroids), although the very smallest are essentially spheres and the very largest (unstable) bubbles are lenticular. To account for the differences in scrubbing and thermal hydraulics, the following formulas are given for basic bubble geometry and gravity settling, oblate spheroids, centrifugal forces, and diffusional deposition.

Basic Bubble Geometry

The necessary for formulas are commonly found in handbooks. For the bubble of elliptical cross-section in Figure 2, the parameters and equations used in SPARC are defined as

a = major axis
b = minor axis
R_a = a/b, ratio

$$e^2 = 1 - b^2/a^2 = 1 - \left(\frac{1}{R_a}\right)^2 = \text{eccentricity}^2 \qquad (3.33)$$

$$V = \frac{4}{3}\pi a^2 b = \frac{\pi D^3}{6} \quad (D = \text{equivalent sphere diameter}) \qquad (3.34)$$

$$A_s = 2\pi a^2 + \frac{\pi b^2}{e} \ln\left[\frac{(1+e)}{(1-e)}\right] = \text{surface area} \qquad (3.35)$$

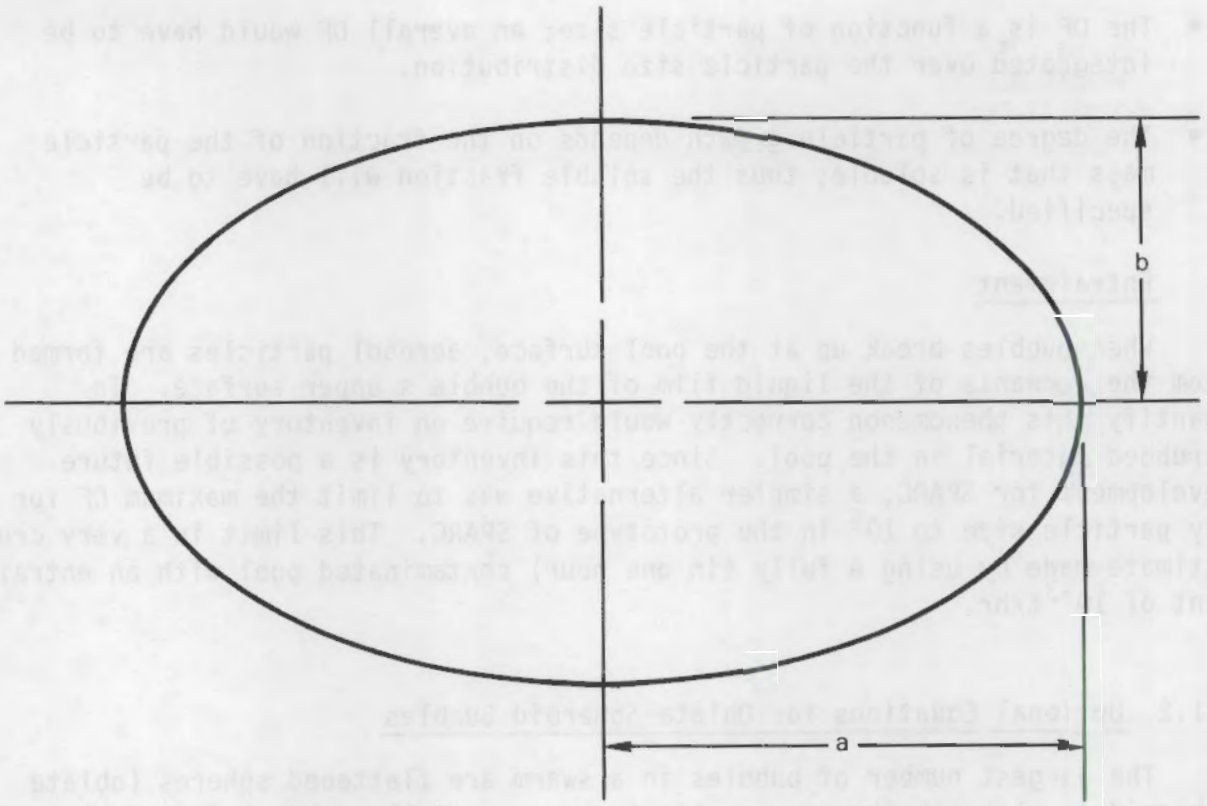

FIGURE 2. Basic Ellipse Axes

Gravity Settling for Oblate Spheroids

The K_s for an oblate spheroid can be approximated using a flattened cylinder of circular, cross-sectional area πa^2. The net depositional velocity on this circular area is $v_s - v_v$, so that the value for K_s is:

$$K_s = \pi a^2 (v_s - v_v)/V$$

$$= \frac{3}{2} (v_s - v_v)(R_a)^{2/3}/D \qquad (3.36)$$

This does not reduce to the spherical form when $R_a \to 1$, but it is close. It reduces exactly if $v_v = 0$.

Centrifugal Forces in an Oblate Spheroid

Because the oblate spheroid has a smaller radius of curvature at the bubble edges than does a sphere of equivalent volume, the General Electric Company has developed a detailed analysis of the enhanced removal by the oblate spheroid bubble. Although their work is not in the open literature, it is

adopted here with their permission.(a) The essence of their development can be applied as a multiplier of the average drift velocity v_c (see Equation 3.18) for a sphere. Thus the average drift velocity for an oblate spheroid is:

$$v_c' = y^* v_c \tag{3.37}$$

where

$$y^* = 4.221\ (R_a) - 6.232 \text{ for } R_a > 3 \tag{3.38}$$

$$y^* = 0.9444\ (R_a)^2 - 1.0776 R_a + 1.1332 \text{ for } R_a < 3 \tag{3.39}$$

are determined as curve fits to their calculated data. From this the K_c for oblate spheroids is:

$$K_c = A_s(y^* v_c - v_v)/V \tag{3.40}$$

which represents the final equation for centrifugal removal of particles. This first order correction could be improved by detailed integrals of the local drift velocity minus v_v over the whole surface.

Diffusional Deposition for an Oblate Spheroid

Equations developed for a sphere are now adjusted for the oblate spheroid geometry. For the larger surface area, the surface element will be exposed for a longer time, t_e, which is now

$$t_3 = 2a/V_b \tag{3.41}$$

When this is incorporated into the velocity for penetration, then

$$V_D' = V_D/(R_a^{1/6}) \tag{3.42}$$

Then from Equation (3.29),

$$\phi_{AB} = \frac{v_v}{V_D'} = \frac{v_v}{V_D}\ (R_a^{1/6}) \tag{3.43}$$

(a) Thanks for this information are due to Dr. Frederick J. Moody, consultant to G.E.'s Nuclear Energy Business Operation, and his colleagues.

which is applied to Equation (3.28). Thus the final result for a new K_D gives

$$K_D = \frac{A_s}{V} V_D' \tag{3.44}$$

Thus the corrections for the three deposition mechanisms have been made for the oblate spheroid to obtain corrected rate constants for gravity settling--Equation (3.36), centrifugal forces--Equation (3.40), and diffusional deposition--Equation (3.44). The vapor velocity v_v for both spheres and oblate spheroids is treated in Section 3.2.2.

3.2 THERMAL-HYDRAULIC MODELS

Because the magnitude of the steam evaporation velocity, which impedes particle capture, depends strongly on the pool temperature, a first-estimate model was derived to predict equilibrium pool temperature. Second, a model for predicting the steam evaporation velocity into rising bubbles was required to quantify the impact on particle deposition.

3.2.1 Equilibrium Pool Temperatures

An energy balance written on the pool may be expressed as

$$\underset{\text{input rate}}{G_i h_i + Q} = \underset{\text{output rate}}{G_o h_o + (G_o - G_i) h_c} + \underset{\text{accumulation rate}}{\frac{d}{dt}(Mh_1)} \tag{3.45}$$

where G = gas flow rate, moles/s
h = specific enthalpy of the gas
h_c = specific enthalpy change due to evaporation
M = total mass of water in the pool
h_1 = specific enthalpy of pool liquid
Q = decay heat rate due to fission products contained in pool water
i,o = subscripts referring to inlet and outlet gas, respectively.

A number of simplifying assumptions were made to obtain an estimate of the equilibrium pool temperature:

1. Specific enthalpy is expressible as a product of heat capacity and temperature difference: $h = C_p(T - T_R)$.

2. The reference temperature was set equal to 0°C.

3. dM/dt was negligible.

4. Gases leaving the pool were saturated with water vapor and in thermal equilibrium with pool water.

5. Pool temperature was everywhere the same.

6. Pool temperature was constant, i.e., dT/dt = 0.

7. The noncondensible gas entering the pool was hydrogen.

8. The mole fracture of entering hydrogen was a specified input variable.

The simplified energy balance equation that results from the listed assumptions is expressible as:

$$\frac{Q}{G_{H_2}} + T_i \left[C_{pH_2} + \frac{(1 - X)}{X} C_{pH_2O}\right] - T_o \left[C_{pH_2} + \frac{\frac{P_w}{P_T} C_{pH_2O}}{1 - \frac{P_w}{P_t}}\right] \tag{3.46}$$

$$- h_c \left[\frac{\left(\frac{P_w}{P_T}\right)}{\left(1 - \frac{P_w}{P_T}\right)} - \frac{(1 - X)}{X}\right] = 0$$

where Q = decay energy, watts
G_{H_2} = H_2 inflow rate, moles/s
T_i = inlet gas temperature, °C
C_{pH_2} = average molar heat capacity of hydrogen, joule/mole °C
C_{pH_2O} = average molar heat capacity of water vapor, joule/mole °C
X = mole fraction of hydrogen in inlet gas
T_o = temperature of outlet gas and pool water, °C
P_T = total atmospheric pressure above pool, atm
P_w = vapor pressure of water at pool temperature, atm
h_c = latent heat of evaporation, cal/mole.

Equation (3.40) was solved numerically to yield a value of T_o that caused the sum to add to zero. Examples of predicted temperatures (made for Q = 3 MW, G_{H_2} = 0.068 kg mole/s, and P_T = 1 atm) are listed in Table 2.

TABLE 2. Equilibrium Temperature of Suppression Pool

Inlet Gas Temperature T_i, °C	Mole Fraction of Hydrogen X	Equilibrium Temperature T_o, °C
1000	1.0	77.4
500	1.0	68.0
1000	0.5	90.7
500	0.5	87.6
1000	0.1	98.3
500	0.1	97.8

As indicated by the data of Table 2, pool temperatures for a so-called saturated pool could be considerably lower than the normal boiling point. Because the evaporation velocity is a strong function of pool temperature in the vicinity of the boiling point, it is important to have realistic estimates of pool temperatures.

Although the illustration is for hydrogen gas, users of SPARC can mix any ratio of steam, hydrogen, air, carbon dioxide, and carbon monoxide.

3.2.2 Steam Evaporation Model

A rising bubble containing noncondensible gases in the suppression pool always tends toward thermal and vapor equilibrium states. The thermal equilibrium is an easy concept to understand; vapor equilibrium is not. For an isothermal bubble to be in vapor equilibrium in the pool both at depth h and at the top, the vapor pressure of water must be the same. To maintain constant vapor pressure, the bubble must receive vapor from the liquid pool as it rises. This vapor flux can hinder particle deposition, and therefore evaporation is important.

Potential for Evaporation

To quantitatively understand the driving forces, a number of definitions are necessary.

Let N_n = noncondensible moles per bubble
D_h = bubble diameter at depth h (for equivalent sphere)
D_s = bubble diameter at surface
P_w = water vapor pressure

P_s = total pressure at surface
N_v = moles of vapor in bubble at h
N_v^s = moles of vapor in bubble at surface
ρ = pool liquid density.

For comparison, the equilibrium states of mole fraction of vapor at depth h and at the pool surface are

$$Y_h = \frac{N_v}{N_v + N_n} = \frac{P_w}{P_s + \rho gh} \qquad \text{(at depth h)} \qquad (3.47)$$

and

$$Y_s = \frac{N_v^s}{N_v^s + N_n} = \frac{P_w}{P_s} \qquad \text{(at the surface)} \qquad (3.48)$$

Solving for N_v^h and N_v^s gives

$$N_v^h = N_n P_w/(P_s + \rho gh - Pw) \qquad (3.49)$$

$$N_v^s = N_n P_w/(P_s - P_w) \qquad (3.50)$$

Clearly $N_v^s > N_v^h$ for all situations of $N_n > 0$ and $h > 0$. If the atmosphere above the pool is pure vapor, then $N_v^s \to \infty$. The potential for evaporation is very high, but there are limitations. First, the energy for evaporation must come from the pool, and second, both heat and mass transfer resistances exist across the bubble/liquid interface. Therefore, the maximum amount of vapor that a bubble can pick up depends on the wall-to-bubble interior vapor pressure difference, the heat transfer resistances across the bubble interface, the mass transfer resistance across the vapor side of the interface, and the bubble rise time. These are examined quantitatively in the following section.

Rate Equations for Evaporation

The basic rate equation for a rising bubble with a circulating surface is based on penetration theory already presented in the discussion of diffusion deposition (Section 3.1). A slightly different application of that theory will be used for both heat and mass transfer here. A variation on Equation (3.19) needed here for mass transfer is

$$W_v = 2 \left[\frac{D_{vB}}{\pi t_e}\right]^{1/2} (C_{vo} - C_{vb}) \qquad (3.51)$$

where W_v is the average flux of vapor into the bubble. Other definitions are

C_{vo} = vapor concentration at the interface = P_w/R
C_{vb} = bulk bubble vapor concentration = N_v/V
D_{vB} = molecular diffusivity of vapor in noncondensible gas B.

The principal heat transfer resistance to vaporization is across the liquid film outside the bubble. It would obey a relationship similar to Equation (3.51),

$$q = 2 \left[\frac{\alpha}{\pi t_e}\right]^{1/2} \pi C_p (T_b - T_o) \qquad (3.52)$$

where q is the average heat flux to the interface (neglecting sensible heat transfer in the bubble). Also in this equation:

α = water thermal diffusivity
C_p = water heat capacity
T_b = bulk pool temperature
T_o - interface temperature.

The next step is to equate q with the change in vapor in the bubble; i.e.

$$A_s q = \lambda_v \frac{dn_v}{dt} \qquad (3.53)$$

and finally

$$A_s N_v = \frac{dn_v}{dt} \qquad (3.54)$$

Equations (3.51) and (3.52) can now be solved for W_v and T_b. Other relationships for pressure, bubble diameter, and rise velocity are needed to complete the SPARC calculations at any time during a bubble's rise period.

The final relationship to get the steam velocity is to divide the wall flux W_v by the molar density at the conditions of the interface.

$$v_v = W_v/(Mw(P_s + P_w)/RT_o) \qquad (3.55)$$

With this definition of v_v, all of the necessary mathematical parts have been defined or used in SPARC. Here Mw is the average molecular weight (of the gas and vapor) at the surface.

One aspect of SPARC that needs to eventually be improved is the overall thermal balance on the bubble. This will include sensible heat transfer across the bubble interface, adiabatic cooling of the bubble upon rising to lower pressures, and possible fog formation caused by the adiabatic cooling.

4.0 SPARC OPERATING REQUIREMENTS

Program SPARC needs only a modest input data file to run cases. The most difficult part is judging the bubble size and shape that will appropriately match the pool conditions. The present version of SPARC allows only one initial bubble diameter and one ratio of major axis/minor axis per run. It is planned that future versions will allow for a spectrum of initial sizes and shape descriptions.

The following sections are intended to help the user to understand the basic operations within SPARC and to operate SPARC with desired accident conditions. Example problems input files are given along with summaries of the expected outputs.

4.1 FLOW DIAGRAM/ALGORITHMS

The flow diagram in Figure 3 portrays SPARC calculations. The user specifies pool and incoming gas composition and conditions at various times. SPARC interpolates between these conditions at the desired output times. The output times correspond to the times when a bubble of specified size and shape carrying the particle loadings and gases rises to the top of the pool. SPARC calculates the DF per particle size and a DF for the overall particle spectrum. Then the exiting particle size distribution is specified in log normal distribution parameters.

One major decision the user must make is whether to use the equilibrium pool temperature or to use some other independent input pool temperature. SPARC calculates the equilibrium pool temperature that is desired. Pool temperature is extremely important when it is near the boiling point. When the pool is at the boiling point, the vapor flux velocity, v_v, is the largest.

4.2 INPUT VARIABLES

The sets of input variables are divided according to type and defined in the following discussions.

4.2.1 Particle Size

Incoming particle sizes are not read in for each case run, but rather are listed in a DATA/DPART statement. See lines 12 to 14 in the listing in the Appendix for the present set of 20 particle size "brackets" used to span the distribution of inlet particles. The user will have to change the DATA/DPART statement to change the size brackets listed.

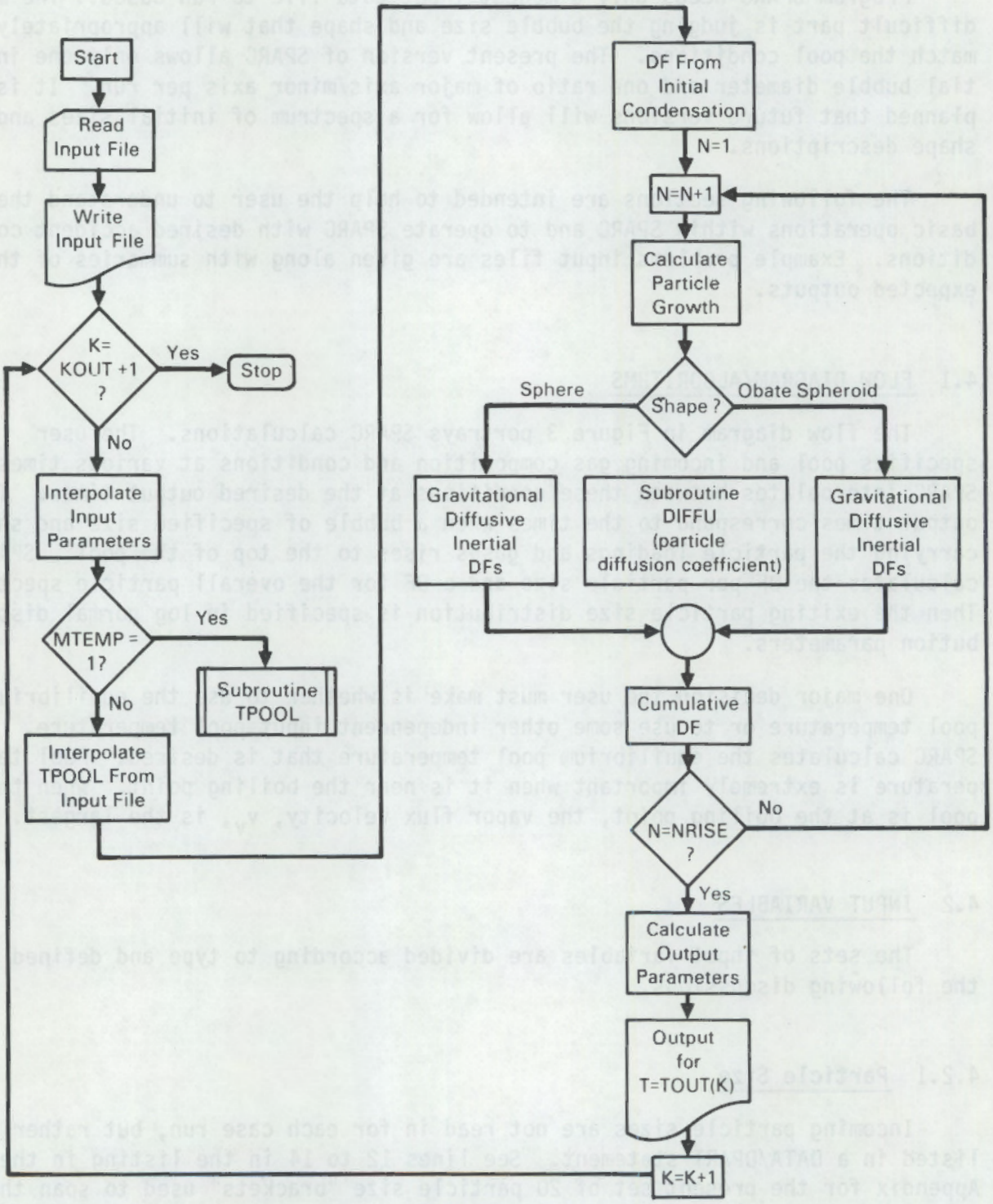

FIGURE 3. SPARC Flow Diagram

4.2.2 Time-Dependent Input Data

If gas flows or compositions, particles characteristics, and pool temperatures change during a run, you will probably want to pick a number of time points where the variables discussed below are given new values. The number of points used for data entry is NOATA = 1, ... 50. You are not likely to be able to use 50 points because of input field space limitation. The time values corresponding to the NDATA are TI (J), in minutes, J = 1, ... NOATA.

Table 3 lists the variables for each NDATA.

Note that if equilibrium pool temperature option is not used, then POOLT(J) must be supplied and the input variables QDECAY(J) are not needed.

Other input data related to time are TCPD, HPD1, HPD2, KOUT, and TOUT(k). These are defined in Table 4.

TABLE 3. SPARC Time-Dependent Variables for Each NDATA

Name	Range	Variable	Units
RHO(J)	J=1, NDATA	Individual particle density	g/cc
SOLF(J)	J=1, NDATA	Weight fraction of soluble material as CsOH	--
PARCON(I,J)	J=1, NDATA I=1, 20	Particle concentration in each size class I	g/cc
H2DOT(J)	J=1, NDATA	Hydrogen gas input rate into pool	g/s
H2ODOT(T)	J=1, NDATA	Water vapor input rate into pool	g/s
CODOT(T)	J=1, NDATA	Carbon monoxide gas rate into pool	g/s
AIRDOT(J)	J=1, NDATA	Air rate into pool	g/s
CO2DOT(J)	J=1, NDATA	Carbon dioxide rate into pool	g/s
TGASIN(J)	J=1, NDATA	Input gas temperature	°C
PGASIN(J)	J=1, NDATA	Input gas pressure	atm absolute
POOLT(J)	J=1, NDATA	Pool temperature	°C
POOLP(J)	J=1, NDATA	Pressure above pool	atm absolute
QDECAY(J)	J=1, NDATA	Isotope decay heat in pool	watts

TABLE 4. Other SPARC Time-Related Variables

Name	Range	Variable	Units
TCPD	--	Time to switch to new pool scrub depth	min
HPD1	--	First scrub depth	cm
HPD2	--	Second scrub depth at TCPD	cm
KOUT	1, 100	Number of desired output times	--
TROT(k)	k=1, KOUT	Specified output times	min

4.2.3 Other Input Data

The remaining input data are defined in Table 5.

Table 5 completes the input variable description. The next section shows a typical input file and corresponding output.

4.3 EXAMPLE PROBLEMS

For illustration purposes, a simple example problem is shown using SPARC. This is followed by an example of the effects of parametric change of bubble shape on scrubbing effectiveness.

4.3.1 Saturated Pool Scrubbing Example

For the case of a saturated pool (100°C, 1 atm), with hot hydrogen gas carrying insoluble particles into the pool for 60 minutes at constant conditions, and for oblate spherical bubbles (RATIO = 4) and DIAM = 0.5 cm, the following input file (Figure 4) was used to obtain only one printout at 30 minutes.

Figure 5 shows the input file listed by variable by SPARC. The values here should be compared to Figure 4 values to help gain familiarity with the input file.

SPARC output is in two parts. Part one (Figure 6) contains the details of each particle size in the pool. Note that the maximum DF = 10^5 is imposed on any particle size. This was done to account for surface entrainment effects. Part two (Figure 7) gives the overall pool performance and log normal distribution parameters of the leaving particles.

TABLE 5. Other SPARC Input Variables

Name	Range	Variable Function
NRISE	1, ...	Numbers of time steps for calculation of DFs during bubble rise
	10-1000	10 < NRISE < 1000 for accuracy
MSHAPE	1 or 2	MSHAPE = 1 to use spherical bubble equations MSHAPE = 2 to use oblate spheroid bubble equations
RATIO	> 1	Ratio of major to minor axes on the ellipitcal section (along the vertical axis) of an oblate spheroid bubble
DIAM	--	Diameter of the equivalent spherical bubble at entrance depth, in centimeters
MTEMP	1 or 2	MTEMP = 1 to use equilibrium pool temperature calculations MTEMP = 2 to use the specified pool temperature PDOLT(J) calculations
MTB	0 or 1	MTB = 0 involves interior heat transfer calculations in the bubble - NOT RECOMMENDED NOW MTB = 1 equates the bulk bubble and bubble surface temperatures
DIAGN	< or > NRISE	DIAGN < NRISE calls for additional parameter information during bubble rise DIAGN > NRISE bypasses this feature
DHV	--	Heat of vaporization of water at the most likely pool temperature DHV = 40 630 joule/g mole is ordinarily adequate
CPPOOL	--	Heat capacity of the pool at the most likely pool temperature CPPOOL = 4.2 joule/g °C is ordinarily adequate

```
2
0.,60.
1.,1.
.0,.0
0.,0.
.59E-9,.59E-9
.59E-7,.59E-7
.117E-5,.117E-5
.588E-5,.588E-5
.137E-4,.137E-4
.231E-4,.231E-4
.166E-4,.166E-4
.465E-5,.465E-5
.744E-6,.744E-6
.693E-7,.693E-7
.31E-8,.31E-8
0.,0.
0.,0.
0.,0.
0.,0.
0.,0.
0.,0.
0.,0.
0.,0.
1400.,1400.
0.,0.
1000.,1000.
1.35,1.35
0.,0.
0.,0.
0.,0.
100.,100.
1.,1.
3.E+6,3.E+6
100.,366.,366.,1,10,2,2,1,4.2,4.063E+04,.5,4.
30.
11
$PRINT SPARC.COM
```

FIGURE 4. Input Data File for Saturated Pool Scrubbing Example (4.3.1)

```
NDATA=          2
TI(I)= 0.0000000E+00     60.00000
RHO(I)=  1.000000         1.000000
SOLF(I)= 0.0000000E+00   0.0000000E+00
PARCON(J,I)= 0.0000000E+00   0.0000000E+00
PARCON(J,I)= 5.8999999E-10   5.8999999E-10
PARCON(J,I)= 5.9000001E-08   5.9000001E-08
PARCON(J,1)= 1.1700000E-06   1.1700000E-06
PAFCON(J,I)= 5.8800001E-06   5.8800001E-06
PARCON(J,I)= 1.3700000E-05   1.3700000E-05
PARCON(J,I)= 2.3099999E-05   2.3099999E-05
PARCON(J,I)= 1.6600001E-05   1.6600001E-05
PARCON(J,I)= 4.6499999E-06   4.6499999E-06
PARCON(J,I)= 7.4399998E-07   7.4399998E-07
PARCON(J,I)= 6.9300000E-08   6.9300000E-08
PARCON(J,I)= 3.1000000E-09   3.1000000E-09
PARCON(J,I)= 0.0000000E+00   0.0000000E+00
PARCON(J,I)= 0.0000000E+00   0.0000000E+00
PARCON(J,I)= 0.0000000E+00   0.0000000E+00
PARCON(J,I)= 0.0000000E+00   0.0000000E+00
PARCON(J,I)= 0.0000000E+00   0.0000000E+00
PARCON(J,I)= 0.0000000E+00   0.0000000E+00
PARCON(J,I)= 0.0000000E+00   0.0000000E+00
PARCON(J,I)= 0.0000000E+00   0.0000000E+00
H2DOT(I) = 1400.000        1400.000
H2OOOT(I)= 0.0000000E+00   0.0000000E+00
TGASIN(I)=  1000.000        1000.000
PGASIN(I)=  1.350000        1.350000
CODOT(I)= 0.0000000E+00   0.0000000E+00
CO2DOT(I)= 0.0000000E+00   0.0000000E+00
AIRDOT(I)= 0.0000000E+00   0.0000000E+00
POOLT(I)=  100.0000        100.0000
POOLP(I)=  1.000000        1.000000
QDECAY(I)   3000000.        3000000.
TCPD=  100.0000
HPDI=  366.0000
HPD2=  366.0000
KOUT=          1
NRISE=         10
MSHAPE=         2
MTEMP=          2
MTB=         1
CPPOOL=  4.200000
DHV=  40630.00
DIAM= 0.5000000
RATIO=  4.000000
TOUT(I)   30.00000
DIAGN=         11
```

FIGURE 5. SPARC Listing of Input Data File for Saturated Pool Scrubbing Example (4.3.1)

Particle Bin Number	Particle Diam Dry (CM)	Particle Diam Wet (CM)	Grams Per Sec Dry	Grams Per Sec Wet	Number Per Sec	Decon. Factor of
1	0.8580E-05	0.8580E-05	0.0000E+00	0.0000E+00	0.0000E+00	0.1241E+01
2	0.1424E-04	0.1424E-04	0.2940E-01	0.2940E-01	0.1945E+14	0.1087E+01
3	0.2360E-04	0.2360E-04	0.3091E+01	0.3091E+01	0.4491E+15	0.1034E+01
4	0.3920E-04	0.3920E-04	0.4513E+02	0.4513E+02	0.143iE+16	0.1405E+01
5	0.6500E-04	0.6500E-04	0.5213E+02	0.5213E+02	0.3625E+15	0.6111E+01
6	0.1078E-03	0.1078E-03	0.1035E+01	0.1035E+01	0.1578E+13	0.7172E+03
7	0.1788E-03	0.1788E-03	0.1251E-01	0.1251E-01	0.4181E+10	0.1000E+06
8	0.2960E-03	0.2960E-03	0.8993E-02	0.8993E-02	0.6623E+09	0.1000E+06
9	0.4920E-03	0.4920E-03	0.2519E-02	0.2519E-02	0.4040E+08	0.1000E+06
10	0.8160E-03	0.8160E-03	0.4031E-03	0.4031E-03	0.1417E+07	0.1000E+06
11	0.1354E-02	0.1354E-02	0.3754E-04	0.3754E-04	0.2888E+05	0.1000E+06
12	0.2240E-02	0.2240E-02	0.1679E-05	0.1679E-05	0.2854E+03	0.1000E+06
13	0.3720E-02	0.3720E-02	0.0000E+00	0.0000E+00	0.0000E+00	0.1000E+06
14	0.6180E-02	0.6180E-02	0.0000E+00	0.0000E+00	0.0000E+00	0.1000E+06
15	0.1026E-01	0.1026E-01	0.0000E+00	0.0000E+00	0.0000E+00	0.1000E+06
16	0.1702E-01	0.1702E-01	0.0000E+00	0.0000E+00	0.0000E+00	0.1000E+06
17	0.2820E-01	0.2820E-01	0.0000E+00	0.0000E+00	0.0000E+00	0.1000E+06
18	0.4680E-01	0.4680E-01	0.0000E+00	0.0000E+00	0.0000E+00	0.1000E+06
19	0.7760E-01	0.7760E-01	0.0000E+00	0.0000E+00	0.0000E+00	0.1000E+06
20	0.1288E+00	0.1288E+00	0.0000E+00	0.0000E+00	0.0000E+00	0.1000E+06

FIGURE 6. SPARC Output (Part One) for Saturated Pool Scrubbing Example (4.3.1)

```
RESULTS FOR 4.00/1 OBLATE SPMEROIDS
0.1000E+01DRY PARTICLE DENSITY (GM/CM**3)
.1000E+01 WET PARTICLE DENSITY (GM/CM**3)
.0000E=00 WEIGHT FRACTION WATER IN PARTICLES
.1906E-04 NUMBER MEDIAN PARTICLE RAOIUS OF DRY PARTICLES (CM)
.1906E-04 NUMBER MEDIAN PARTICLE RADIUS OF NET PARTICLES (CM)
.1379E+01 GEOMETRIC STANOARD DEVIATION OF DRY PARTICLES
.1379E+01 GEOMETRIC STANDARO OEVIATION OF WET PARTICLES
.3574F+04 TOTAL GRAMS/SEC DRY PARTICLES INTO POOL
.1014E+03 TOTAL GRAMS/SEC DRY PARTICLES LEAVING POOL
.1014E+03 TOTAL GRAMS/SEC WET PARTICLES LEAVING POOL
.1000E+03 POOL TEMPERATURE (DEGREES CELSIUS)
.7717E+02 EQUILIBRIUM POOL TEMPERATURE (DEGREES CELSIUS)
.1000E+01 PRESSURE ABOVE POOL (ATM)
.9900E+02 RELATIVE HUMIDITY OF GAS LEAVING POOL (PERCENT)
```

FIGURE 7. SPARC Output (Part Two) for Saturated Pool Scrubbing Example (4.3.1)

4.3.2 Parameteric Effects of Bubble Shape

To help the user of SPARC appreciate the parametric sensitivity of bubble shape on scrubbing results, a series of four runs was carried out using the conditions of the previous example except for pool temperature, which for this case is 20°C. Figure 8 is a plot of log DF versus log (dry particle diameter) for values of RATIO = 1, 2, 3, and 4. Note that for the spherical bubble, maximum penetration occurs at a particle size of ~0.4 μm and DF = 1.75. DFs are much larger at RATIO = 4 with maximum penetration at a particle size of

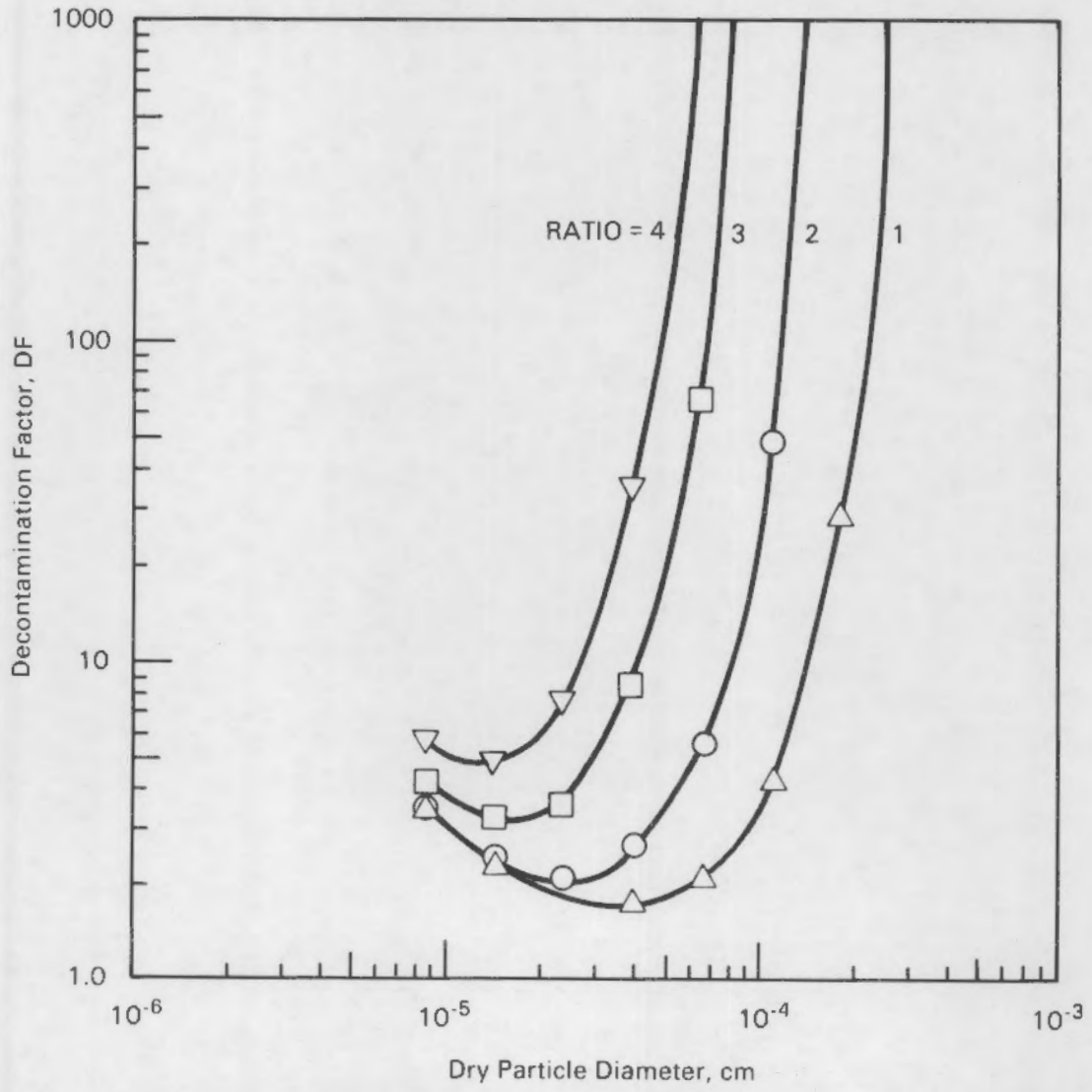

FIGURE 8. Comparison of DF Versus Dry Particle Size for a 0.5-cm Bubble at Different Ratios of Major/Minor Axes

0.16 μm and DF = 5. The overall DF on a spectrum of particles will be even more pronounced than that of the maximum penetration size. Thus, the user should approach selection of RATIO with caution. Until experimental evidence gives quantitative information on this selection to represent a whole swarm of bubble shapes, the user might select for a gas inlet condition with high water content (over 50% by volume). The bubbles will be smaller (< 0.5 cm) and more spherical (RATIO of 1 to 2), whereas a dry gas will give larger (> 0.5 cm) and more eccentric bubbles (RATIO of 3 to 4).

5.0 REFERENCES

Bird, R. B., W. E. Stewart and E. N. Lightfoot. 1960. Transport Phenomena, John Wiley and Sons, Inc., New York, NY.

Calderback, P. H., and A. C. Lochiel. 1964. "Mass Transfer Coefficients, Velocities and Shapes of Carbon Dioxide Bubbles in Free Rise Through Distilled Water." Chemical Engineering Science. 19:485-503.

Crank, J., 1967. The Mathematics of Diffusion. Oxford University Press, London.

Fletcheer, N. H. 1962. The Physics of Rainclouds. Cambridge University Press, London.

Fuchs, N. H. 1964. The Mechanics of Aerosols. The MacMillan Company, New York, NY.

Gieseke, J. A., P. Cybulskis, R. S. Denning, M. R. Kuhlman and K. W. Lee. 1984. Radionuclide Release Under Specific LWR Accident Conditions. Volume II, BWR Mark I Design, Volume III, BWR Mark III Design. BMI-2104 DRAFT, Battelle Columbus Laboratories, Columbus, OH.

Li, P., et al. 1965. "Unsteady State Mass Transfer from Gas Bubbles - Liquid Phase Resistance." AICHE Journal, 11(4):581-587.

APPENDIX

CODE LISTING FOR PROTOTYPIC VERSION OF SPARC

APPENDIX

CODE LISTING FOR PROTOTYPIC VERSION OF SPARC

```
      DRAFT VERSION OF CODE SPARC IN DEVELOPMENT
C     TO CALCULATE SUPPRESSION POOL AEROSOL REMOVAL
C
c     This code has been prepared in contemplation of Commission action.
c     It may not have received patent review and may contain information
c     received in confidence.  Therefore, the contents of this code
c     should neither be disclosed to others nor reproduced wholly or
c     partially, unless written permission to do so has been obtained
c     from the appropriate U.S. NRC office.  The recipient is requested
c     to take the necessary action to ensure the protection of this code.
c     The distribution of the computer code is governed by the 'industrial
c     property of a proprietary nature' clause of the Article on 'Use of
c     Information' of the Agreement on Severe Fuel Damage Research Partic-
c     ipation.  This Article limits the dissemination which can be made by
c     the receiving party.
C
      INTEGER DIAGN
      DIMENSION TI(50),DPART(20),RHO(50),SOLF(50),PARCON(20,50)
     1 ,H2DOT(50),H2ODOT(50),TGASIN(50),PGASIN(50),CODOT(50),
     2 AIRDOT(50),CO2DOT(50),POOLT(50),POOLP(50),QDECAY(50),
     3 PMDOT(20),PRCON(20),DFOV(20),Y(5),VS(5),WM(5),Z(5),PHI(5,5),
     4 VSET(20),DFG(20),DFD(20),DIF(20),DFO(20),DFOV(20),DFC(20)
     5 ,OPMDOT(20),AMD(20),AN(20),DPARTW(20),WPMDOT(20),TOUT(100)
      DATA DPART/.858E-5,.1424E-4,.236E-4,.392E-4,.650E-4,.1078E-3,
     1 .1788E-3,.296E-3,.492E-3,.816E-3,.1354E-2,.224E-2,.372E-2,
     2 .618E-2,.1026E-1,.1702E-1,.282E-1,.468E-1,.776E-1,.1288/
C
C     SPARC INPUT VARIABLES
C
C     NDATA = 1,.....,50 MAX , NUMBER OF TIME POINTS FOR DATA ENTRY
C     TI(J),J=1,NDATA , TIME VALUES AT EACH NDATA (MINUTES)
C     DPART(I),I=1,.....,20 CHARACTERISTIC DIAMETER OF EACH OF 20
C              PARTICLE BUCKETS (CM)
C     RHO(J),J=1,NDATA , PARTICLE DENSITY (G/CC)
C     SOLF(J),J=1,NDATA , WEIGHT FRACTION SOLUBLE MATERIAL
C     PARCON(I,J)       , PARTICLES IN EACH SIZE CLASS (G/CC)
C     H2DOT(J)          , HYDROGEN INTO POOL (G/SEC)
C     H2ODDT(J)         , WATER (G/SEC)
C     TGASIN(J)         , INPUT GAS TEMPERATURE (C)
C     PGASIN(J)         , INPUT GAS ABSOLUTE PRESSURE (ATM)
C     CODOT(J)          , CARBON MONOXIDE (G/SEC)
C     AIRDOT(J)         , AIR (G/SEC)
C     CO2DOT(J)         , CARBON DIOXIDE (G/SEC)
C     POOLT(J)          , POOL TEMP. AT J (C)
C     POOLP(J)          , PRESSURE ABOVE POOL (ATM)
C     QDECAY(J)         , DECAY POWER IN POOL (WATTS)
C     TCPD              , TIME TO SWITCH TO NEW SCRUB DEPTH
C     HPD1              , FIRST SCRUB DEPTH , STARTING AT T=0
C     HPD2              , LAST SCRUB DEPTH , STARTING AT T=TCPD
C     KOUT=1,.....,100  , NUMBER OF OUTPUT STEPS
C     TOUT(K),K=1,....,KOUT  , SPECIFIED OUTPUT TIMES (MIN)
```

```
C       DIAGN (INTEGER) IS FOR INTERMEDIATE PRINT OUTS WHICH OCCUR EVERY
C       'DIAGN' TIME STEPS.  IF NO INTERMEDIATE PRINTS ARE DESIRED SET
C       'DIAGN' GREATER THAN 'NRISE'.
C
C
C       READ INPUT DATA
C
        OPEN(UNIT=4,NAME='SPARC.DAT',TYPE='OLD',READONLY)
        READ(4,*)NDATA                                    ! INPUT LINE 1
        PRINT * , 'NDATA=',NDATA
        READ(4,*)(TI(I),I=1,NDATA)                        ! INPUT LINE 2
        PRINT * , 'TI(I)=',(TI(I),I=1,NDATA)
        READ(4,*)(RHO(I),I=1,NDATA)                       ! INPUT LINE 3
        PRINT * , 'RHO(I)=',(RHD(I),I=1,NDATA)
        READ(4,*)(SOLF(I),I=1,NDATA)                      ! INPUT LINE 4
        PRINT * , 'SOLF(I)=',(SOLF(I),I=1,NDATA)
        DO 5 J=1,20
        READ(4,*)(PARCON(J,I),I=1,NDATA)                  ! INPUT LINES 5 THRU 24
5       PRINT * , 'PARCON(J,I)=',(PARCON(J,I),I=1,NDATA)
        READ(4,*)(H2DOT(I),I=1,NDATA)                     ! INPUT LINE 25
        PRINT * , 'H2DOT(I)=',(H2DOT(I),I=1,NDATA)
        READ(4,*)(H2ODOT(I),I=1,NDATA)                    ! INPUT LINE 26
        PRINT * , 'H2ODOT(I)=',(H2ODOT(I),I=1,NDATA)
        READ(4,*)(TGASIN(I),I=1,NDATA)                    ! INPUT LINE 27
        PRINT * , 'TGASIN(I)=',(TGASIN(I),I=1,NDATA)
        READ(4,*)(PGASIN(I),I=1,NDATA)                    ! INPUT LINE 28
        PRINT * , 'PGASIN(I)=',(PGASIN(I),I=1,NDATA)
        READ(4,*)(CODOT(I),I=1,NDATA)                     ! INPUT LINE 29
        PRINT * , 'CODOT(I)=',(CODOT(I),I=1,NDATA)
        READ(4,*)(CO2DOT(I),I=1,NDATA)                    ! INPUT LINE 30
        PRINT * , 'CO2DOT(I)=',(CO2DOT(I),I=1,NDATA)
        READ(4,*)(AIRDOT(I),I=1,NDATA)                    ! INPUT LINE 31
        PRINT * , 'AIRDOT(I)=',(AIRDOT(I),I=1,NDATA)
        READ(4,*)(POOLT(I),I=1,NDATA)                     ! INPUT LINE 32
        PRINT * , 'POOLT(I)=',(POOLT(I),I=1,NDATA)
        READ(4,*)(POOLP(I),I=1,NDATA)                     ! INPUT LINE 33
        PRINT * , 'POOLP(I)=',(POOLP(I),I=1,NDATA)
        READ(4,*)(QDECAY(I),I=1,NDATA)                    ! INPUT LINE 34
        PRINT * , 'QDECAY(I)=',(QDECAY(I),I=1,NDATA)
C
C       MTB=1 FOR TB.EQ.TS
C       MTB=0 FOR TB.NE.TS
C       MTEMP=1 FOR TW.NE.POOLTT
C       MTEMP=0 FOR TW.EQ.POOLTT
C
C
C                                                         ! INPUT LINE 35
        READ(4,*)TCPD,HPD1,HPD2,KOUT,NRISE,MSHAPE,MTEMP,MTB,CPPOOL,DHV
        PRINT * ,'TCPD=',TCPD
        PRINT * , 'HPD1=',HPD1
        PRINT * , 'HPD2=',HPD2
```

```
      PRINT * , 'KOUT=',KOUT
      PRINT * , 'NRISE=',NRISE
      PRINT * , 'MSHAPE=',MSHAPE
      PRINT * , 'MTEMP=',MTEMP
      PRINT * , 'MTB=',MTB
      PRINT * , 'CPPOOL=',CPPOOL
      PRINT * , 'DHV=',DHV
      READ(4,*)(TOUT(I),I=1,KOUT)                          ! INPUT LINE 36
      PRINT * , 'TOUT(I)=',(TOUT(I),I=1,KOUT)
      READ(4,*)DIAGN                                       ! INPUT LINE 37 (END OF
INPUT)
      PRINT * , 'DIAGN=',DIAGN
C
C     RG=82.06 (GAS CONSTANT IN CC ATM/GMOLE-K)
      RG=82.06
      PI=3.14159265
C
C     MASSAGE INPUT DATA
C
C     OETERMINE MOLE FRACTION OF NONCONDENSABLE GASES
C     AND ACTUAL VALUES AT TIME T
C
C     MAJOR COMPUTATION LOOP (TO END OF PROGRAM)
C
      DO 1000 K=1,KOUT
      T=TOUT(K)
      JOUT=NDATA-1
      DO 999 JM=1,JOUT
C
C     THIS LOOP ESTABLISHES INTERPOLATION VALUES
C
      IF(TOUT(K).GE.TI(JM).AND.TOUT(K).LT.TI(JM+1))JIN=JM
999   CONTINUE
      OINT=(TOUT(K)-TI(JIN))/(TI(JIN+1)-TI(JIN))
      DO 998 JP=1,20
      PRCON(JP)=PARCON(JP,JIN)+DINT*(PARCON(JP,JIN+1)-PARCON(JP,JIN))
998   CONTINUE
      RHOT=RHO(JIN)+DINT*(RHO(JIN+1)-RHO(JIN))
      SOLFT=SOLF(JIN)+DINT*(SOLF(JIN+1)-SOLF(JIN))
      H2DT=H2DOT(JIN)+OINT*(H2DOT(JIN+1)-H2DOT(JIN))
      H2ODT=H2ODOT(JIN)+DINT*(H2ODOT(JIN+1)-H2OOOT(JIN))
      CODT=CODOT(JIN)+DINT*(CODOT(JIN+1)-CODOT(JIN))
      CO2DT=CO2DOT(JIN)+OINT*(CO2DOT(JIN+1)-CO2DOT(JIN))
      AIROT=AIRDOT(JIN)+DINT*(AIRDOT(JIN+1)-AIRDOT(JIN))
      POOLTT=POOLT(JIN)+DINT*(POOLT(JIN+1)-POOLT(JIN))
      POOLPT=POOLP(JIN)+DINT*(POOLP(JIN+1)-POOLP(JIN))
      QDK=QDECAY(JIN)+DINT*(QDECAY(JIN+1)-QDECAY(JIN))
      TGAS=TGASIN(JIN)+DINT*(TGASIN(JIN+1)-TGASIN(JIN))
      PGAS=PGASIN(JIN)+DINT*(PGASIN(JIN+1)-PGASIN(JIN))
C
C     CALCULATE GMOLAR FLOW RATE-GMOLES/SEC  (GMDOT)
```

```
      GMDOT=H2DT/2.+H2ODT/18.+CODT/28.+CO2DT/44.+AIRDT/29.
C
C     MOLAR FLOW NONCONDENSABLES-GMOLES/SEC  (GMNC)
C
      GMNC=GMDOT-H2ODT/18.
C
C     MOLE PR. NONCOND (XNC)
C
      XNC=GMNC/GMDOT
C
C     VOLUME FLOW RATE (TOTAL)-CC/SEC  (VDOT)
C
      TABS=TGAS+273.2
      VDOT=GMDOT*RG*TABS/POOLPT
C
C     MASS FLOW RATE INTO POOL BY SIZE OF PARTICLE , PMDOT(I)
C
      DO 997 I=1,20
      PMDOT(I)=VDOT*PRCON(I)
997   CONTINUE
      XCO=(CODT/28.)/GMNC
      XCO2=(CO2DT/44.)/GMNC
      XAIR=(AIRDT/29.)/GMNC
      XH2=(H2DT/2.)/GMNC
C
C     DECONTAMINATION BY EARLY CONDENSATION
C
C     IF XNC=0. , THEN DF=INFINITY IN A WELL MIXED EQUILIBRIUM POOL
C
C     PICK PROPER POOL DEPTH (HPD)
C
      HPD=HPD1
      IF(T.GE.TCPD)HPD=HPD2
      G=980.
      AP=3.2437814
      BP=5.86826E-03
      CP=1.1702379E-08
      DP=2.1878462E-03
      CALL TPOOL(XH2,XCO,XCO2,XAIR,TGAS,POOLPT,XNC,GMNC,QDK,TW)
      IF(MTEMP.NE.1)TW=POOLTT
      TP=TW+273.2
      XP=647.27-TP
      PW=218.167*10.**(-(XP/TP)*(AP+BP*XP+CP*(XP**3.))/(1.+DP*XP))
C
C     XEQ=EQUIL. MOLE FRACTION OF NONCONDENSABLES AT DEPTH HPD
C
      RHPOOL=1.03421-7.59E-04*TW
      IF(TW.LE.100.)RHPOOL=1.02536-6.705E-04*TW
C
C     RHPOOL IN G/CM**3
C
```

```
      PTOT=POOLPT+RHPOOL*HPD*G/1.0132E+06
      XEQ=1.-PW/PTOT
C
C     DF FOR EARLY CONDENSATION = DFEC
C
      IF(XNC.EQ.0.)XNC=1.E-10
      DFEC=XEQ/XNC
      IF(DFEC.LT.1.)DFEC=1.
      WRITE(6,99) DFEC
C
C     BUBBLE RISE CALCULATIONS AND PARTICLE GROWTH
C     NRISE CALCULATIONS CORRESPONDING TO NRISE RISE STEPS
C     OF THE BUBBLE SWARM
C
      VSWARM=116.
C
C     VSWARM IN CM/SEC
C
C     DURATION OF EACH STEP = DS (SECONDS)
      DS=(HPD/VSWARM)/NRISE
C
C     DISTANCE TRAVELED IN DS, HPD/NRISE=DX
C
      DX=HPD/NRISE
C
C     DEFINE NSTEP AS POSITION INDES
C
C
C     FIRST STEP - INITIALIZE
C
C     TMG=TDTAL MDLES OF GAS IN BUBBLE
      DIAM=.5
      TMG=(PI*DIAM**3.)*PTOT/(6.*RG*TP)
      ENV=(1.-XEQ)*TMG
      ENG=XEQ*TMG
C
C     ESTABLISH LENNARD-JONES PARAMETERS
C
      SIGH2=2.915
      EPSH2=38.
      SIGAIR=3.617
      EPSAIR=97.
      SIGCO=3.59
      EPSCO=110.
      SIGCO2=3.996
      EPSCO2=190.
C
C     ASSUME LJ PARAMETERS OF NC GASES ARE LINEAR COMBINATIONS BASED
C     ON MOLE FRACTION
```

```
C
      SIGG=XH2*SIGH2+XCO*SIGCO+XCO2*SIGCO2+XAIR*SIGAIR
      EPSG=XH2*EPSH2+XCO*EPSCO+XCO2*EPSCO2+XAIR*EPSAIR
C
C     EMWG=AVG MOL. WT. NC GASES
C
      EMWG=XH2*2.+XCO*28.+XCO2*44.+XAIR*29.
C
C     FINALLY WITH H2O VAPOR, CALC SIG AND EPS
C
      SIG=0.5*(SIGG+2.641)
      EPS=SQRT(EPSG*809.1)
C
C     TP=POOL TEMP (DEGREES KELVIN)
C     TS=SURFACE OF BUBBLE TEMP(K) AT GIVEN DEPTH
C     TB=INTERIOR BUBBLE TEMP(K) AT A GIVEN DEPTH
C     PT=TOTAL PRESSURE AT GIVEN DEPTH(ATM)
C     P1=PT AT PREVIOUS DEPTH(ATM)
      ALPHA=.1698E-02
      PT=PTOT
      R=82.06
      TB=TP
      RM=(1./18.02+1./EMWG)**.5
      B=0.00214-.000492*RM
      TS=TP
      DO 650 J=1,20
      DFOV(J)=DFEC
650   CONTINUE
C
C     BEGIN BUBBLE RISE CALCULATIONS
C
      DO 499 I=1,20
499   DFOV(I)=DFEC
      DO 500 NR=1,NRISE
      IF(MOD(NR,DIAGN).EQ.0)PRINT * , NR
      P1=PT
C
C     FIRST ESTABLISH BUBBLE GROWTH AND VAPOR VELOCITIES
C
      PT=POOLPT+RHPOOL*(HPD-DX*FLOAT(NR))*G/1.0132E+06
      DIAM=1.2407*(R*TB*(ENG+ENV)/PT)**(.33333)
      VT=17.05882+5.88235*DIAM
C
C     VT=TERMINAL VELOCITY OF BUBBLE (CM/SEC)
C
      OMEGAD=0.7075+0.7341*EPS/TB
      DIFF=B*(TB**1.5)*RM/(PT*OMEGAD*SIG*SIG)
      XPM=647.27-TP
      XP=647.27-TS
      PV=218.167*10.**(-(XP/TS)*(AP+BP*XP+CP*(XP**3.))/(1.+DP*XP))
      PVM=218.167*10.**(-(XPM/TP)*(AP+BP*XPM+CP*(XPM**3.))/
```

```
     1  (1.+DP*XPM))
        IF(PV.GT.PVM)PV=PVM
        PA=(PT+P1)/2.
        XMS=PV/PA
        XMB=ENV/(ENV+ENG)
        IF(XMS.GE.1.)XMS=0.99
        RS=(XMS-XMB)/(1.-XMS)
        IF(XMB.GE.XMS)GO TO 41
        THETA=(ALOG(RS+1.))/RS
        GO TO 40
41      THETA=0.
40      DR=((PV-PA*XMB)*THETA/(R*TS))/(1.-XMS)
        D1=PI*DIAM*DIAM
        IF(MSHAPE.EQ.2)D1=1.42774*D1
C
C       D1=$URFACE AREA OF BUBBLE
C
        D2=SQRT(4.*DIFF*VT/(PI*DIAM))
        IF(MSHAPE.EQ.2)D2=D2/1.25992
        ENT1=ENV+ENG
        ENV2=ENV+D1*D2*DR*DS
        ENT=ENV2+ENG
        XMT=PV/PT
        AMF2=ENV2/ENT
        IF(AMF2.GT.XMT)GO TO 200
        GO TO 210
200     ENV2=XMT*ENG/(1.-XMT)
        ENT=ENV2+ENG
210     CONTINUE
        DENV=ENV2-ENV
        ENV=ENV2
        Q=DHV*DENV/DS
        D3=SQRT(4.*ALPHA*VT/(PT*DIAM))
        IF(MSHAPE.EQ.2)D3=D3/1.25992
        TS=TP-Q/(RHPOOL*CPPOOL*D3*D1)
        IF(TS.GT.TP)TS=TP
C
C       VV=VAPOR VELOCITY (CM/SEC)
C       VDENV=VAPOR FORMED IN DS SECONDS (CM**3)
C
        VDENV=DENV*R*TS/PT
        VV1=VV
        VV=VDENV/(D1*DS)
        IF(VV.LT.0.)VV=0.
C
C       ADIABATIC COOLING CORRECTION
C
        T2=TB*(PT/P1)**.242
        TB=(ENT1*T2+DENV*TS)/(ENT1+DENV)
C
C       TO AVOID ADIABATIC COOLING TB=TS
```

```
C
      IF(MTB.EQ.1)TB=TS
C
C     SATN= SATURATION OF BUBBLE  (RH/100)
C
      XP3=647.27-TB
      PV3=218.167*10.**(-(XP3/TB)*(AP+BP*XP3+CP*(XP3**3.))
     1 /(1.+DP*XP3))
      SATN=AMF2*PT/PV3
      IF(MOD(NR,DIAGN).EQ.0)PRINT * , 'VV=',VV
      IF(MOD(NR,DIAGN).EQ.0)PRINT * , 'TP=',TP,' TS=',TS,' TB=',TB
      IF(MOD(NR,DIAGN).EQ.0)PRINT * , 'SATN=',SATN
C
C     END BUBBLE GROWTH CALCULATION
C
C     START PARTICLE GROWTH CALCULATIONS
C
C     GIVEN:
C     RHOT, DRY PARTICLE DENSITY OF DIAM=DPART(IP)
C     BUBBLE SATURATION = SATN, SOLFT WT. FR. SOLUBLE MATERIAL
C
C     CALCULATE:
C     WET PARTICLE DIAM=DPART(IP)*RDPART
C     AND CORRESPONDING DENSITY WRHO
C
C     PICK DPART=1 CM
C     WMC=MASS OF SOLUTE (AS CSOH)
      WMC=SOLFT*RHOT*PI/6.
C
C     WMS=MASS OF SOLVENT H2O
C     WFWET=FRACTION OF MASS AS H2O
C
      IF(SATN.GE..99)SATN=.99
      WMS=0.24*WMC/(1./SATN-1.)
      VI=(1.-SOLFT)*PI/6.
      RHOS=1.
      IF(WMC.EQ.0.)GO TO 332
      RHOS=1.+1.04*WMC/(WMC+WMS)
332   VS1=(WMC+WMS)/RHOS
      WMI=RHOT*PI/6.
      WRHO=(WMS+WMI)/(VI+VS1)
      RDPART=(6.*(VS1+VI)/PI)**.3333
      WFWET=WMS/(WMI+WMS)
      IF(MOD(NR,DIAGN).EQ.0)PRINT * , 'WFWET=',WFWET
C
C     END PARTICLE GROWTH CALCULATIONS
C
C     NOTE: FOR THE SIZE RANGE TO BE ENCOUNTERED, PARTICLE GROWTH
C     IS THE SAME PROPORTION FOR THE WHOLE SIZE RANGE.
C
C     BEGIN PARTICLE DEPLETION BY GRAVITY SETTLING. DEFINE DFG(IP)
```

```
C       AS DECONTAMINATION FACTOR BY PARTICLE SIZE
C
C       FIRST GET SETTLING VELOCITY, VSET=WRHO*DIAM**26./(18.*VIS)
C       WHERE VIS=BUBBLE GAS VISCOSITY
C
C       LENNARD-JONES APPROACH AGAIN
C
        EPSH2O=809.1
        SIGH2O=2.641
C
C       DEFINE MOLE FRACTIONS WITH STEAM AMF2 MOLE FRACTION
C
        YH2O=AMF2
        YH2=(1.-AMF2)*XH2
        YCO=(1.-AMF2)*XCO
        YCO2=(1.-AMF2)*XCO2
        YAIR=(1.-AMF2)*XAIR
        OMH2O=0.765+0.82*EPSH2O/TB
        VISH2O=2.6693E-05*SQRT(18.*TB)/((SIGH2O**2.)*OMH2O)
        OMH2=0.765+0.82*EPSH2/TB
        OMCO=0.765+0.82*EPSCO/TB
        OMCO2=0.765+0.82*EPSCO2/TB
        OMAIR=0.765+0.82*EPSAIR/TB
        VISH2=2.6693E-05*SQRT(2.*TB)/((SIGH2**2.)*OMH2)
        VISCO=2.6693E-05*SQRT(28.*TB)/((SIGCO**2.)*OMCO)
        VISCO2=2.6693E-05*SQRT(44.*TB)/((SIGCO2**2.)*OMCO2)
        VISAIR=2.6693E-05*SQRT(29.*TB)/((SIGAIR**2.)*OMAIR)
        Y(1)=YH2O
        Y(2)=YH2
        Y(3)=YCO
        Y(4)=YCO2
        Y(5)=YAIR
        VS(1)=VISH2O
        VS(2)=VISH2
        VS(3)=VISCO
        VS(4)=VISCO2
        VS(5)=VISAIR
        WM(1)=18.
        WM(2)=2.
        WM(3)=28.
        WM(4)=44.
        WM(5)=29.
        DO 301 J=1,5
        DO 301 I=1,5
        PHI(I,J)=1./(((1.+WM(I)/WM(J))*8.)**.5)*(1.+SQRT(VS(I)/VS(J))
     1  *(WM(J)/WM(I))**.25)**2
301     CONTINUE
        DO 302 I=1,5
        Z(I)=0.
        DO 302 J=1,5
        Z(I)=Z(I)+Y(J)*PHI(I,J)
```

```
302     CONTINUE
        VISMIX=0.
        DO 303 I=1,5
        VISMIX=VISMIX+Y(I)*VS(I)/Z(I)
303     CONTINUE
C
C       VISMIX IN POISES. CALCULATIONS USE BSL PAGE 24
C
C       CALCULATE SETTLING VELOCITIES NOW (VSET(I))
C       AVG MOL WEIGHT (AMW)
        AMW=0.
        DO 309 J=1,5
        AMW=AMW+Y(J)*WM(J)
309     CONTINUE
        DO 304 I=1,20
        CALL DIFFU(DPART(I),RDPART,VISMIX,TP,AMW,PTOT,DIFUS,CM)
        VSET(I)=WRHO*G*CM*(DPART(I)*RDPART)**2./(18.*VISMIX)
C
C       FOLLOWING TAKEN FROM BNWL-1326, PAGE 12-13
C
        RHOGAS=AMW*PT/(RG*TP)
        FDRE2=1.3333*WRHO*RHOGAS*G*((RDPART*DPART(I))**3.)/(VISMIX**2.)
        IF(FDRE2.GT.9.6.AND.FDRE2.LT.93.6)RE=(FDRE2/27.)**(1./1.13)
        IF(FORE2.GE.93.6.AND.FDRE2.LT.410.)RE=(FDRE2/24.32)**(1./1.227)
        IF(FDRE2.GE.410..AND.FDRE2.LT.1.07E+04)RE=(FDRE2/15.71)**
     1  (1./1.417)
        IF(FDRE2.GE.1.07E+04.AND.FDRE2.LT.2.45E+05)RE=(FDRE2/6.477)
     1  **(1./1.609)
        IF(FDRE2.GE.2.45E+05)RE=(FDRE2/1.194)**(1./1.867)
        IF(FDRE2.GT.9.6)VSET(I)=RE*VISMIX/(DPART(I)*RDPART*RHOGAS)
C
        IF(MOD(NR,DIAGN).EQ.0)PRINT * , 'VSET(I)=',VSET(I),' FDRE2=',
     1  FDRE2,' RE=',RE
304     CONTINUE
C
C       BEGIN REMOVAL MECHANISMS DURING BUBBLE RISE
C
C       START WITH GRAVITY SETTLING
C
        DO 305 N=1,20
        ADF=DS*(1.5*VSET(N)-VV)/DIAM
        IF(ADF.GT.12.)ADF=12.
        DFG(N)=EXP(ADF)
        VIG=1.5*VSET(N)/DIAM
C
C       FOR AN OBLATE SPHEROID OF ECCENTRICITY=4, USE BELOW
C
        BDF=DS*(VSET(N)-VV)*3.78/DIAM
        IF(BDF.GT.12.)BDF=12.
        IF(MSHAPE.EQ.2)DFG(N)=EXP(BDF)
        IF(DFG(N).LT.1.)DFG(N)=1.
```

```
C
C       CONTINUE WITH CENTRIFUGAL (INERTIAL) DEPOSITION
C
        VC=((PI*VT)**2.)*VSET(N)/(2.*G*DIAM)
        CDF=(6.*DS/DIAM)*(VC-VV)
        VIC=(6./DIAM)*VC
        IF(CDF.GT.12.)CDF=12.
        DFC(N)=EXP(CDF)
C
C       FOR AN OBLATE SPHERIOD, DF=EXP(A*DS), WHERE A (ELLIPSE 4/1)
C       10.44*A(SPHERE)
C
        DDF=(6.*DS/DIAM)*(10.44*VC-VV)
        IF(DDF.GT.12.)DDF=12.
        IF(MSHAPE.EQ.2)DFC(N)=EXP(DDF)
        IF(DFC(N).LT.1.)DFC(N)=1.
C
C       CONTINUE WITH DIFFUSIONAL DEPOSITION
C
        CALL DIFFU(DPART(N),RDPART,VISMIX,TP,AMW,PTOT,DIFUS,CM)
        DIF(N)=DIFUS
        VD=2.*SQRT(DIF(N)*VT/(PI*DIAM))
        VID=6.*VD/DIAM
        PHID=VV/(VD*PI**.5)
        IF(PHID.GT.5.)GO TO 400
        THETAD=EXP(-PHID**2.)/(2.-EXP(-1.85*PHID))
        DFDN=6.*THETAD*VD*DS/DIAM
        DFD(N)=EXP(DFDN)
        PHID=1.26*PHID
        THETA2=EXP(-PHID**2.)/(2.-EXP(-1.85*PHID))
        DFDONT=1.8*DFDN*THETA2/THETAD
        IF(MSHAPE.EQ.2)DFD(N)=EXP(DFDONT)
        GO TO 401
400     DFD(N)=1.
401     IF(DFD(N).LT.1.)DFD(N)=1.
C
C       OVERALL OF FOR TIME STEP DS,DFO(N)
C
        IF(ADF.EQ.12..OR.BDF.EQ.12..OR.CDF.EQ.12..DR.DDF.EQ.12.)
     1  GO TO 333
        IF(DFO(N).EQ.0.) GO TO 334
        ABC=ALOG(DFO(N))+ALOG(DFOV(N))
        IF(ABC.GT.12.)GO TO 333
334     DFO(N)=DFG(N)*DFC(N)*DFD(N)
C
C       OVERALL DF FOR BUBBLE TO THIS POINT, DFOV(N)
C
        DFOV(N)=DFO(N)*DFOV(N)
        GO TO 335
333     DFO(N)=1.E+5
        DFOV(N)=1.E+5
```

```
335      IF(MOD(NR,DIAGN).EQ.0)PRINT * , 'N=',N,' DFG(N)=',DFG(N),
     1' DFC(N)=',DFC(N),' DFD(N)=',DFD(N),' DFO(N)=',DFO(N),' =',DFOV(N)
     1  ,DFOV(N)
         IF(MOD(NR,DIAGN).EQ.0)PRINT * , 'VIG=',VIG,' VIC=',VIC,' VID='
     1  ,VID
         IF(MOD(NR,DIAGN).EQ.0)PRINT * , 'DPART(N)=',DPART(N),' RDPART='
     1  ,RDPART,' DIF(N)=',DIF(N),' CM=',CM,' VISMIX=',VISMIX,' DS=',DS
     2  ,' VT=',VT,' DIAM=',DIAM,' TP=',TP,' AMW=',AMW
305      CONTINUE
500      CONTINUE
C
C        END BUBBLE RISE CALCULATIONS
C
C        PREPARE OUTPUT INFFORMATION
C
C        FLOWRATE OF DRY PARTICLE SIZE() OUT OF POOL, (OPMDOT(I)) AND
C        WET(WPMDOT(I)) AND TOTAL FLOWRATE OF PARTICLES (TFPO/TPFI)
         TFPI=0.
         TFPO=0.
         DO 310 I=1,20
         OPMDOT(I)=PMDOT(I)/DFOV(I)
         WPMDOT(I)=OPMDOT(I)/(1.-WFWET)
         TFPI=TFPI+PMDOT(I)
         TFPO=TFPO+OPMDOT(I)
310      CONTINUE
         WTFPO=TFPO/(1.-WFWET)
C
C        WTFPO = TOTAL FLOWRATE OF WET PARTICLES
C
C        OUTPUT PARTICLE NUMBERS/SEC = AN(N)
C        MASS OF DRY PARTICLE, AMD(N)
C
         ANT=0.
         DO 311 I=1,20
         AMD(I)=RHOT*PI*(DPART(I)**3.)/6.
         AN(I)=OPMDOT(I)/AMD(I)
C
C        ANT = TOTAL NUMBER FLOWRATE
C
         ANT=ANT+AN(I)
311      CONTINUE
C
C        ANMEND = NO. MEAN PARTICLE DIAM: DRY
C        ANMENW = NO. MEAN PARTICLE DIAM: WET
C        ANMEDD = NO. MEDIAN PARTICLE DIAM: DRY
C        ANMEDW = NO. MEDIAN PARTICLE DIAM: WET
         ANMEND=0.
         ANMENW=0.
         ANMEDD=0.
         ANMEDW=0.
         DO 312 I=1,20
```

```
      DPARTW(I)=DPART(I)*RDPART
      ANMEDD=ANMEOD+AN(I)*ALOG(DPART(I))
      ANMEDW=ANMEDW+AN(I)*ALOG(OPARTW(I))
      ANMEND=ANMENO+AN(I)*DPART(I)
      ANMENW=ANMENW+AN(I)*DPART(I)*RDPART
312   CONTINUE
      ANMEDW=EXP(ANMEDW/ANT)
      ANMEDD=EXP(ANMEOO/ANT)
      ANMEND=ANMENO/ANT
      ANMENW=ANMENW/ANT
C
C     CALCULATE:
C     SIGWET = GEOMETRIC STD DEVIATION OF WET PARTICLES
C     SIGDRY = GEOMETRIC STO DEVIATION OF DRY PARTICLES
C
      SWET=0.
      SDRY=0.
      DO 313 N=1,20
      SWET=SWET+AN(N)*((ALOG(DPARTW(N)/ANMENW))**2.)
      SORY=SDRY+AN(N)*((ALOG(DPART(N)/ANMEND))**2.)
313   CONTINUE
      SIGWET=EXP((SWET/ANT)**.5)
      SIGDRY=EXP((SORY/ANT)**.5)
      RAODRY=ANMEDD/2.
      RAOWET=ANMEDW/2.
      CALL TPOOL(XH2,XCO,XCO2,XAIR,TGAS,POOLPT,XNC,GMNC,QDK,TW)
      RELH=SATN*100.
      TPOL=TP-273.2
      WRITE(6,100)K,TOUT(K)
      OO 10 I=1,20
      WRITE(6,101)I,DPART(I),DPARTW(I),OPMDOT(I),WPMDOT(I),AN(I),
     1  DFOV(I)
10    CONTINUE
      IF(MSHAPE.NE.2)WRITE(6,102)
      IF(MSHAPE.EQ.2)WRITE(6,103)
      WRITE(6,104)RHOT,WRHO,WFWET,RAODRY,RAOWET,SIGDRY,SIGWET,TFPI,
     1  TFPO,WTFPO,TPOL,TW,POOLPT,RELH
1000  CONTINUE
99    FORMAT(1H1,T12,'DECONTAMINATION FACTOR BY EARLY CONDENSATION= ',
     1  E10.4,/)
100   FORMAT(1HO,' TOUT(',I3,')=',F7.2,' MINUTES. MATERIALS LEAVING',
     1  ' POOL',///,' PARTICLE',T15,'PARTICLE',T30,'PARTICLE',T46,
     2  'GRAMS',T61,'GRAMS',T75,'NUMBER',T90,'OECON.',/,'   BIN',
     3  T16,'DIAM',T31,'DIAM',T45,'PER SEC',T60,'PER SEC',T75,
     4  'PER SEC',T90,'FACTOR',/,' NUMBER',T15,'DRY (CM)',T30,
     5  'WET (CM)',T46,'DRY',T61,'WET',T90,'DF',/)
101   FORMAT(1H T3,I2,T15,6(E10.4,5X))
102   FORMAT(1H1,' RESULTS FOR SPHERICAL BUBBLES')
103   FORMAT(1H1,' RESULTS FOR 4/1 OBLATE SPHEROIDS')
104   FORMAT(1HO,E10.4,T12,'DRY PARTICLE DENSITY (GM/CM**3)',/,
     1  E10.4,T12,'WET PARTICLE DENSITY (GM/CM**3)',/,
```

```
     2  E10.4,T12,'WEIGHT FRACTION WATER IN PARTICLES',/,
     3  E10.4,T12,'NUMBER MEDIAN PARTICLE RADIUS OF DRY PARTICLES (CM)'
     4  ,/E10.4,T12,'NUMBER MEDIAN PARTICLE RADIUS OF WET PARTICLES(CM)'
     5  ,/,E10.4,T12,'GEOMETRIC STANDARD DEVIATION OF DRY PARTICLES',
     6  /,E10.4,T12,'GEOMETRIC STANDARD DEVIATION OF WET PARTICLES',
     7  /,E10.4,T12,'TOTAL GRAMS/SEC DRY PARTICLES INTO POOL',/,
     8  E10.4,T12,'TOTAL GRAMS/SEC DRY PARTICLES LEAVING POOL',/,
     9  E10.4,T12,'TOTAL GRAMS/SEC WET PARTICLES LEAVING POOL',/,
     1  E10.4,T12,'POOL TEMPERATURE (DEGREES CELCIUS)',/,
     2  E10.4,T12,'EQUILIBRIUM POOL TEMPERATURE (DEGREES CELCIUS)',/,
     3  E10.4,T12,'PRESSURE ABOVE POOL (ATM)',/,
     4  E10.4,T12,'RELATIVE HUMIDITY OF GAS LEAVING POOL (PERCENT)')
        STOP
        END
        SUBROUTINE DIFFU(DPART,RDPART,VISMIX,TP,AMW,PT,DIFUS,CM)
C
C       THIS SUBROUTINE CALCULATES PARTICLE DIFFUSIVITY, DIF(N)
C       AS A FUNCTION OF PARTICLE SIZE
C
C       INPUTS:
C       DPART, RDPART, VISMIX, TP, AMW
C
C       CUNNINGHAM FACTOR, CM AND ELAM, MEAN FREE PATH OF GAS
C
        PI=3.14159265
        ELAM=1.245E-02*((TP/AMW)**.5)*VISMIX/PT
        DPA=DPART*RDPART
        RATD=ELAM/DPA
        CM=1.+2.492*RATD+0.84*RATD*EXP(-0.435/RATD)
        DIFUS=1.38E-16*TP*CM/(3.*PI*VISMIX*DPA)
C
C       OUTPUT: DIFFUSIVITY,DIFUS IN CM**2/SEC
C
        RETURN
        END
        SUBROUTINE TPOOL(XH2,XCO,XCO2,XAIR,TGAS,POOLPT,XNC,GMNC,QDK,TW)
C
C       INPUT TO TPOOL
C
C       XH2      H2 MOLE FRACTION IN INERT GAS
C       XCO      CO MOLE FRACTION IN INERT GAS
C       XCO2     CO2 MOLE FRACTION IN INERT GAS
C       XAIR     AIR MOLE FRACTION IN INERT GAS
C       TGAS     INLET GAS TEMP. (C)
C       POOLPT   PRESSURE ABOVE POOL (ATM)
C       XNC      MOLE FRACTION INERT GAS IN INPUT
C       GMNC     GMOLES/SEC INERT GAS
C       QDK      DECAY HEAT RATE (WATTS)
C
C       OUTPUT FROM TPOOL = POOL TEMP (C) = TW
C
```

```
      DTW1=10.
      TW1=20.
      IF(XNC.EQ.0.)GO TO 797
799   TW1=TW1+DTW1
C
C     HEAT OF WATER VAPORIZATION (JOULES/GMOLE)
C
      DHVAP=40626.
C
C     VAPOR PRESS WATER AT TW - PV (ATM)
C
      AP=3.2437814
      BP=5.86826E-3
      CP=1.1702379E-8
      DP=2.1878462E-3
C
C     CALCULATE AVERAGE HEAT CAPACITIES (JOULE/GMOLE-C)
C
801   T1=TW1+273.2
      XP=647.27-T1
      PV=218.167*10.**(-(XP/T1)*(AP+BP*XP+CP*(XP**3.))/
     1  (1.+DP*XP))
      T0=273.2
      CPH2O=7.7+(2.297E-4*(T1**2.-T0**2.)+8.402E-7*(T1**3.-T0**3.)
     1  -2.1468E-10*(T1**4.-T0**4.))/(T1-T0)
      CPH2O=4.184*CPH2O
      CPH2=6.952+(-2.288E-4*(T1**2.-T0**2.)
     1  +3.1877E-7*(T1**3.-T0**3.)-5.1975E-11*(T1**4.-T0**4.))/(T1-T0)
      CPH2=4.184*CPH2
      CPAIR=6.713+(2.3485E-4*(T1**2.-T0**2.)
     1  +3.8233E-7*(T1**3.-T0**3.)-1.174E-10*(T1**4.-T0**4.))/(T1-T0)
      CPAIR=4.184*CPAIR
      CPCO=6.726+(2.E-4*(T1**2.-T0**2.)
     1  +4.2767E-7*(T1**3.-T0**3.)-1.3268E-10*(T1**4.-T0**4.))/(T1-T0)
      CPCO=CPCO*4.184
      CPCO2=5.316+(7.1425E-3*(T1**2.-T0**2.)-2.7873E-6*(T1**3.-T0**3.)
     1  +4.46E-10*(T1**4.-T0**4.))/(T1-T0)
      CPCO2=CPCO2*4.184
      CPMIX=XH2*CPH2+XCO*CPCO+XCO2*CPCO2+XAIR*CPAIR
C
C     ITERATIVE EQUATIONS BELOW
C
      C1=TGAS*(CPMIX+(1-XNC)*CPH2O/XNC)
      PR=PV/POOLPT
      C2=CPMIX+PR*CPH2O/(1.-PR)
      C3=DHVAP*(PR/(1.-PR)-(1.-XNC)/XNC)
      C4=QDK/GMNC
      TW2=(C1+C4-C3)/C2
      IF(TW2.GT.TW1)GO TO 799
      IF(ABS(TW2-TW1).LE..2)GO TO 798
      TW1=TW1-DTW1
```

```
      DTW1=DTW1/10.
      GO TO 799
797   B=3.87872E+3
      A=11.7466
      TW1=-230.2-B/(ALOG(P)-A)
      GO TO 798
C
C     END ITERATIVE CALCULATIONS
C
798   CONTINUE
      TW=TW1
      RETURN
300   END
```

DISTRIBUTION

No. of Copies

OFFSITE

U.S. Nuclear Regulatory Commission
Division of Technical Information and Document Control
7920 Norfolk Ave.
Bethesda, MD 20014

R. M. Bernero
Office of Nuclear Reactor Regulation
U.S. Nuclear Regulatory Commission
Washington, DC 20555

R. O. Meyer
Office of Nuclear Regulatory Research
U.S. Nuclear Regulatory Commission
Washington, DC 20555

J. A. Mitchell
U.S. Nuclear Regulatory Commission
Washington, DC 20555

5 C. W. Nilsen
Office of Nuclear Regulatory Research
U.S. Nuclear Regulatory Commission
Washington, DC 20555

M. Silberberg
Office of Nuclear Regulatory Research
U.S. Nuclear Regulatory Commission
Washington, DC 20555

No. of Copies

K. G. Steyer
Office of Nuclear Regulatory Research
U.S. Nuclear Regulatory Commission
Washington, DC 20555

J. A. Gieseke
Battelle Columbus Laboratory
505 King Avenue
Columbus, OH 43201

R. Oehlberg
Electric Power Research Institute
P.O. Box 10412
Palo Alto, CA 94303

M. R. Kuhlmann
Electric Power Research Institute
P.O. Box 10412
Palo Alto, CA 94303

K. W. Lee
Electric Power Research Institute
P.O. Box 10412
Palo Alto, CA 94303

D. D. Paul
Electric Power Research Institute
P.O. Box 10412
Palo Alto, CA 94303

R. C. Vogel
Electric Power Research Institute
P.O. Box 10412
Palo Alto, CA 94303

No. of Copies

A. K. Postma
Route 1
Box 46A
Halfway, OR 97834

A. T. Wassel
Science Applications, Inc.
2615 Pacific Coast Highway,
Suite 300
Hermosa Beach, CA 90254

J. E. Brockmann
Sandia National Laboratories
P.O. Box 5800
Albuquerque, NM 87185

M. W. Jankowski
International Atomic Energy
Agency
Wagramerstrasse 5
P.O. Box 100
A-1400 Vienna, Austria

A. Ludewig
Bldg. 130
Brookhaven National Laboratory
Upton, NY 11973

Wen-Shi Yu
Bldg. 130
Brookhaven National Laboratory
Upton, NY 11973

K. W. Holtzclaw
General Electric Co.
175 Curtner Avenue
San Jose, CA 95125

D. A. Hankins
General Electric Co.
175 Curtner Avenue
San Jose, CA 95125

No of Copies

C. N. Amos
General Electric Co.
175 Curtner Avenue
San Jose, CA 95125

H. E. Townsend
General Electric Co.
175 Curtner Avenue
San Jose, CA 95125

D. D. Jones
General Electric Co.
175 Curtner Avenue
San Jose, CA 95125

ONSITE

Westinghouse Hanford Company

R. K. Hilliard
L. D. Muhlestein

33 Pacific Northwest Laboratory

W. J. Apley
D. W. Dragnich
L. D. Kannberg
W. W. Laity
N. S. Laulainen
P. C. Owczarski (10)
A. M. Sutey
W. K. Winegardner (10)
Technical Information (5)
Publishing Coordination (2)

NRC FORM 335 (11-81)

U.S. NUCLEAR REGULATORY COMMISSION

BIBLIOGRAPHIC DATA SHEET

1. REPORT NUMBER (Assigned by DDC)
NUREG/CR-3317
PNL-4742

4. TITLE AND SUBTITLE (Add Volume No., if appropriate)
Technical Bases and User's Manual for the Prototype of SPARC - A Suppression Pool Aerosol Removal Code

2. (Leave blank)

3. RECIPIENT'S ACCESSION NO.

7. AUTHOR(S)
P.C. Owczarski
A. K. Postma
R. I. Schreck

5. DATE REPORT COMPLETED
MONTH: April YEAR: 1985

9. PERFORMING ORGANIZATION NAME AND MAILING ADDRESS (Include Zip Code)
Pacific Northwest Laboratory
P. O. Box 999
Richland, WA 99352

DATE REPORT ISSUED
MONTH: May YEAR: 1985

6. (Leave blank)

8. (Leave blank)

12. SPONSORING ORGANIZATION NAME AND MAILING ADDRESS (Include Zip Code)
Division of Engineering Technology
Office of Nuclear Regulatory Research
U. S. Nuclear Regulatory Commission
Washington, D.C. 20555

10. PROJECT/TASK/WORK UNIT NO.

11. FIN NO.
B2444

13. TYPE OF REPORT

PERIOD COVERED (Inclusive dates)

15. SUPPLEMENTARY NOTES

14. (Leave blank)

16. ABSTRACT (200 words or less)

The Pacific Northwest Laboratory has developed a prototypic version of a Suppression Pool Aerosol Removal Code (SPARC). This code was written to calculate the capture of aerosol particles in the pressure suppression pool (wet well) of a boiling water reactor under hypothetical accident conditions. The code incorporates five aerosol scrubbing models and two thermal-hydraulic models. The scrubbing models describe 1) steam condensation, 2) soluble particle growth in a humid atmosphere, 3) gravitational settling, 4) inertial deposition, 5) diffusional deposition. Mechanical entrainment of pool liquid by breaking of bubbles at the surface was also considered. An optional model for equilibrium pool temperature and a model for steam evaporation are the two thermal-hydraulic models used in the code. Steam evaporation was found to significantly retard deposition processes in pools near the boiling point.

The code user supplies the values of several controlling variables in the code input. The SPARC output can include the decontamination factors (DF) of twenty different particle size groups, an overall DF for the whole particle distribution, particle log normal distribution parameters, and mass flow rates of particles (wet and dry) leaving the pool.

17. KEY WORDS AND DOCUMENT ANALYSIS

17a. DESCRIPTORS

ESF
engineered safety features
fission product retention
core-melt accidents
pressure suppression pool

17b. IDENTIFIERS/OPEN-ENDED TERMS

18. AVAILABILITY STATEMENT
Unlimited

19. SECURITY CLASS (This report)
Unclassified

21. NO. OF PAGES

20. SECURITY CLASS (This page)
Unclassified

22. PRICE
$

NRC FORM 335 (11-81)